The unravelling of radiocarbon composition of organic carbon in river sediments to document past anthropogenic impacts on river systems

Yoann Copard, Frederique Eyrolle, Cécile Grosbois, Hugo Lepage, Loic Ducros, Amandine Morereau, Nathan Bodereau, Catherine Cossonnet, Marc Desmet

The unravelling of radiocarbon composition of organic carbon in river sediments to document past anthropogenic impacts on river systems

Yoann Copard[1], Frédérique Eyrolle[2], Cécile Grosbois[3], Hugo Lepage[2], Loic Ducros[4], Amandine Morereau[2,5], Nathan Bodereau[2], Catherine Cossonnet[2], Marc Desmet[3]

[1] University of Rouen-Normandie, UMR CNRS 6143 M2C, 76821 Mont Saint Aignan, France.
[2] Institut de Radioprotection et de Sureté Nucléaire (IRSN), PSE-ENV, SRTE/LRTA, SAME/LMRE, BP 3, 13115 Saint-Paul-lez-Durance, France.
[3] University of Tours, EA 6293, laboratoire GéHCO, 37200 Tours, France
[4] University of Nîmes, EA7352 CHROME, Laboratoire GIS, 30035 Nîmes, France.
[5] Sorbonne Université, UMR CNRS 7619 METIS, 75252 Paris, France
corresponding author: Yoann Copard (yoann.copard@univ-rouen.fr)

Highlights

- Aquatic POC in sedimentary archives does not record ^{14}C from the nuclear industry
- $\Delta^{14}C$ values of terrestrial POC as a tool to determine the transit time of sediments within the watershed
- $\Delta^{14}C$ as a useful tool to document the trajectories of social and economic milestones.

Acknowledgement

This work was supported by the Institute for Radioprotection and Nuclear Safety (France) and the NEEDS-Environment funding (PALYNO project, 2017-2018). POC and Palynofacies were performed at the Institut des Sciences de la Terre d'Orléans laboratory. Warm thanks

are addressed to Marielle Hatton, Jean-Paul Bakyono, Franck Giner, David Mourier and Cédric Le Corre for their help during field operation, sample preparation and sample analyses.

The unravelling of radiocarbon composition of organic carbon in river sediments to document past anthropogenic impacts on river systems

ABSTRACT

As carriers of dissolved and particulate loads that connect continental surfaces to oceans, river systems play a major role in the global carbon cycle. Indeed, riverine particulate organic carbon (POC) is a melange of various origins characterized by their own ^{14}C labeling. In addition, civil nuclear activities have brought new ^{14}C source that remains poorly documented. We propose to unravel the $\Delta^{14}C$ value of POC stored in a sedimentary archive collected downstream the most nuclearized European rivers (the Loire River). We postulate that riverine POC is a mixture of aquatic POC (which could be impacted by the liquid discharge from nuclear industry), terrestrial and petrogenic POC. With a combination of radiocarbon measurements, POC analyses and the palynofacies method, we assessed the respective $\Delta^{14}C$ value of the POC origins. The gaps between the $\Delta^{14}C$ values of the sedimentary POC and those of the atmosphere were the result of the dilution from dead-C, the freshwater reservoir effect imprinting the $\Delta^{14}C$ of aquatic POC and the age and transit time of terrestrial POC within the catchment. Importantly, we consider that the unraveling of radiocarbon composition of riverine POC could be useful to determine either the transit time of material from source to sink, some past industrial or natural events, the resilience of the river system and milestones of the social and economic trajectory of a catchment. For the last three decades, riverine sediments could also act as a source of radiocarbon for the atmosphere.

1. INTRODUCTION

Since the peak atmospheric ^{14}C level, which occurred in 1963 after nuclear tests, the atmospheric ^{14}C content has been gradually decreasing mainly due to carbon redistribution within the atmosphere and through oceanic and continental pumping (Levin and Hesshaimer, 2000; Naegler and Levin, 2009). This decrease was disrupted by fossil fuel emissions containing depleted ^{14}C, which exacerbated the decrease in the $^{14}C/^{12}C$ ratio in the atmosphere (Sundquist, 1993; Soon et al., 1999; Levin and Hesshaimer, 2000). As an example, Levin and Hesshaimer (2000) reported that fossil gas emissions contributed to 50% of the reduction in global atmospheric $^{14}CO_2$ levels in the 2000s. These studies also indicate that since the early 1990s, the biospheric organic compartment that was previously subjected to atmospheric global fallout from nuclear tests has redistributed the ^{14}C that was initially trapped due to mineralization processes, constituting a delayed ^{14}C source for the atmosphere.

In rivers, organic carbon (OC), is either associated to suspended particulate matter (i.e. POC, expressed in wt. %) or to sedimentary particles (i.e. sedimentary OC, in wt. %), and comes from various origins, including aquatic organic matter from primary production and terrestrial organic matter from the catchment (soils, superficial formations, sedimentary rocks) delivered to hydrosystems by surface processes (e.g. Marwick et al., 2015). During the photosynthesis pathway that occurs in rivers, the former generally reflects ^{14}C levels ranging from those characterizing the atmosphere to those of the Freshwater Reservoir Effect (FRE) depending on water mass circulation and mixing at the watershed scale (e.g. MacDonald et al., 1987). As a consequence, the radiocarbon concentration in aquatic POC may not be in equilibrium with that of the atmosphere, depending on the levels of dissolved carbonate in water - originating from the weathering of carbonate rocks outcropping in the catchment and / or from groundwater - and may produce CO_2 depleted in ^{14}C (e.g. MacDonald et al., 1987, Ascough et al. 2010); this process is called the hard water-effect (Zhou et al., 2015). In addition, downstream nuclear power plants (NPPs), this aquatic

autochthonous POC, is expected to integrate part of the ^{14}C released by NPPs during photosynthesis and may be theoretically enriched in ^{14}C when compared to atmospheric levels. Terrestrial POC can be divided into three main sources: (i) soil POC (POCs) with various ^{14}C concentrations, (ii) POC from various origins held in superficial formations (more and less aged riverine deposits or colluvium) with various and even depleted ^{14}C concentrations (reworked POC, POCrw), and (iii) petrogenic POC (POCp) devoid of ^{14}C, which originates from sedimentary rocks or sediments older than 60 ky (dead carbon, e.g. Leithold et al., 2006, Copard et al., 2018). The ^{14}C content in both POCs and POCrw vary with the age of the compounds (e.g., Schmidt et al., 2011) and reflect the ^{14}C content of the atmosphere during their photosynthesis. Prior to its deposition, terrestrial POC, including the petrogenic part, is subjected to different processes occurring in the catchment. These are related to the connectivity of the landscape compartments, as portrayed by the sediment cascade concept (e.g. Fryirs et al., 2007) and to an unknown number of deposition and resuspension cycles during the lateral transport in rivers, as depicted by the POC spiraling concept (Newbold et al. 1982). All these more and less time-consuming processes promote the mineralization of the riverine POC and increase its mean aging. In summary, the higher the residence time of terrestrial POC in the watershed, the greater ~~the~~ probability of enhancing its mineralization and subsequent CO_2 evasion (Raymond et al., 2013).

Generally, river sediments essentially consist of detrital material of various grain sizes, driven by the local hydrodynamic conditions, and include evidence of past aquatic primary production. However, sedimentary OC stored in rivers mainly originates from the catchment since (i) the chemical and physical properties of the terrestrial POC make it more recalcitrant than POCa to further degradation both in the water column and during early diagenesis (e.g., Hedges et al., 1997) and (ii) the suspended load rapidly limits aquatic primary production in river systems (e.g., Meybeck, 2006). As a consequence, sedimentary archives can be viewed as a mixture of all these POC sources, with rather a terrestrial (e.g. from the catchment) imprint. The ^{14}C measurements performed on bulk sedimentary OC reflect such mixing and each source is characterized by its own ^{14}C labelling.

As a consequence, the question of the nature of organic material isolated for further isotopic measurements of ^{14}C levels is crucial and clearly depends on the scientific question and field. As an example, for paleo-environmental issues, ^{14}C activity is mostly measured from organic particles consisting of wood debris, seeds or charcoals extracted from marine, lacustrine or riverine sediments to date materials (e.g., Dezileau et al., 2014). However in sediment archives, some of these organic particles, such as wood debris, may not be suitable for building an age model and assessing sedimentation rates due to the so-called "old wood effect" which lead to aging processes (cf. inbuilt age, Gavin, 2001). Such a bias can also arise when focusing on refractory organic material, such as charcoals, because of their long residence times in the catchment either in river-banks, soils or sediments located upstream of the studied sedimentary deposit (Oswald et al., 2005). However, for these refractory materials, ^{14}C ages are suitable for deciphering the biomass fire or fossil fuel origins of black carbon (Wang et al., 2016). For understanding soil dating and soil C dynamics, ^{14}C analyses are performed on either bulk soil OM (Rumpel et al, 2002) or their related specific organic compounds, or fractions, which were previously isolated after substantial and time-consuming physical, chemical and/or biological extraction (e.g. Trumbore, 2009). Lastly in coastal and marine environments, ^{14}C analyses coupled with analyses other isotopes ($\delta^{13}C$) can constitute a powerful method of defining the age and the origin of organic particles in water column or in in sediments (i.e. aquatic, terrestrial, fossil, black carbon, e.g. Bauer et al., 2001). For specific marine OM, such ostracods, and with respect to the age reservoir of marine water, ^{14}C measurements can be viewed as a powerful method of dating marine sedimentary deposits (e.g. Berndt et al., 2019).

In this study, without any pretreatments to isolate specific organic compounds, we aim to unravel the ^{14}C contents in sedimentary OC held by decadal fluvial deposits located downstream of the nuclearized Loire River (France), by considering the relative amounts of various POC components. Such refinement is expected to highlight the ^{14}C origins and the

relative contributions of the various ^{14}C sources, including potential imprints from the nuclear industry.

2. BACKGROUND, METHODS AND ANALYSES

2.1. Coring site characteristics, sampling and age model

The studied sediment core was previously described in Eyrolle et al. (2019). Briefly, several 1 m long sedimentary archives were collected near Montjean-sur-Loire (France) on September 2016 (0 ° 51'23.1 "W - 47 ° 23'34.0" N; Altitude: 13 m) on the right bank of an island in the Loire River, just upstream of the estuary influence and downstream of the last NPP (Figure 1). Several 1m long-cores were sampled within a $1m^2$ area using a percussion corer (Cobra TT - SDEC) with tubes 45 mm in diameter in order to collect enough material. Once collected, the cores were transported to the laboratory where 5 cm slices were sampled along the core and immediately stored at -25°C. Then, the samples were separately freeze-dried under dehydrated nitrogen flux to avoid any atmospheric exchange before analyses. This coring site is one of the most well known in the Loire basin as it is based on a previous and very fine study of a sediment core collected in the same site in 2009 where grain size, mineralogical and geochemical proxies have been detailed (Grosbois et al, 2012). In this previous work, the anthropogenic history of the Loire sediments during the XX^{th} century has been evidenced. The main findings showed a wide range of contamination patterns resulting from the urban development, ore-processing and related activities but also from an important river eutrophication leading to endogenic calcite precipitation and a dilution effect of contaminant contents. For this study, sedimentological parameters (fig. 2A and B) show clayey-silty sediments all along the 1-m core with an uniform particle size distribution (80% of silts) and a D_{50} ranging from 15 to 28 μm. Only sediment layers at the bottom show some variations with a finer layer at 110 cm deep cm deep and a coarser one below 120 cm cm. All these variations make each core comparable to the one studied previously (Grosbois et al, 2012) and, as any significant geomorphological and sedimentological changes

occurred for the past 10 years, this present work benefits of information from the 2 previous studies (Grosbois et al, 2012; Eyrolle et al, 2019).

The age model was based on radiocesium and $^{238}Pu/^{239+240}Pu$ ratio (Fig. 2C). Radiocesium concentrations with depth show two major peaks at 92.5 cm and 37.5 cm. These peaks are associated to peaking radioactive emissions from atmospheric nuclear tests in 1963 and to fallout from the Chernobyl accident in 1986, respectively, and can be used as chronological signals (fig. 2). The radiocesium peak in 1986 is preceded from 67.5 cm of depth to 37.5 cm by relatively high radiocesium concentrations due to the liquid discharges by the Loire river NPPs gradually implanted since 1957 (UNGG then PWR of Chinon NPP's) then from the beginning of 80's for the WPR. Furthermore, $^{238}Pu/^{239+240}Pu$ activity ratios (fig. 2) also show two maximums, one at 77.5 cm depth (0.06±0.01), the other at 52.5 cm (0.08±0.01). Plutonium isotopes initially results from the atmospheric fallout due to nuclear tests performed over 1945-1980 mainly in the northern Hemisphere and from atmospheric deposition related to the explosion of the Transit 5 BN-3 satellite over the Indian Ocean in 1964. In the particular case of the Loire River, plutonium activity ratios significantly higher than those characterizing the atmospheric reference values are dur to the accidental liquid plutonium discharges in 1969 and 1980 at the Saint-Laurent-Les-eaux NPP's. Thus, $^{238}Pu/^{239+240}Pu$ activity ratio peaks constitute, in addition to the radiocesium peaks, additional chronological markers for dating the archive. From these chronological landmarks (1963, 1669, 1980, 1986 and 2016), a simplified age model was applied connecting years and depths. All these results for the age model using ^{137}Cs and plutonium isotopes were previously published (Eyrolle et al., 2019) and demonstrated ~~show~~ that the 1 m long archive covers almost the last seven decades (1950–2016) with constant sedimentation rates over two main periods, the 1963–1986 period with 2.4 ± 0.2 cm/y and the 1986–2016 one with1.3 ± 0.2 cm/y as expected from Grosbois et al. (2012).

2.2. Origins of Particulate Organic Carbon in rivers

As shown in Figure 3, sedimentary OC can be viewed as a mixture of POCs from soil, reworked POCrw from superficial deposits, POCp from sedimentary rock and POCa from aquatic primary productivity. The three former components originate from the catchment and are considered as detrital. In particular, POCrw is part of the sedimentary cascade within the catchment (e.g. Fryirs et al., 2007) and is stored in superficial formations such as colluvium, terraces, sediments deposited upstream of the studied station and/or even ancient soils. As a consequence, POCrw consists of a mixture of various types of aged POC. POCa, POCs and POCrw correspond to biospheric POC (POCb) since the age of POCrw can be younger than 60 ky (Brugeron et al., 2018). These two latter components are considered a part of terrestrial POC (POCt). However, an unknown part of POCrw could be devoid of ^{14}C and could also be assimilated into POCp. Among all these components, POCa is the one that is able to reflect liquid radiocarbon releases from the nuclear industry. All these sources exhibit a large range of $\Delta^{14}C$ and $\delta^{13}C$ values, with a possible overlap when these two isotopes are combined to decipher the origins of the POC pool and their cycling (fig. 4, modified from Marvick et al., 2015 see also section 2.4). A convenient simplification considers that ~~P~~OC, either in sediments or in suspended particulate matter (POC), can be seen as a binary mixture of dead-C POC (i.e. POCp and some POCrw) and POC from the biosphere showing a mean ^{14}C activity (Leithold et al., 2006). This binary mixture concept is frequently used to extract POCp from POC or sedimentary OC but suggests that the two end-members fulfil three requirements: the mean OC content and the ^{14}C concentration in POCb must remain globally constant as the POCp content (Galy et al., 2008). At first glance, and as seen in the figure 4, the large range of $\Delta^{14}C$ and $\delta^{13}C$ values for the different sources able to supply riverine POC implies that the use of this binary mixture remains unreliable. However, if we consider that (i) the intensity of erosion processes in the catchment is variable with space and (ii) the catchment is at the equilibrium state in terms of the climatic, anthropogenic and geological variables ruling erosion, then only some specific sedimentary sources preferentially supply the river (Walling, 1983). Hence, the use of this binary mixture remains a reasonable compromise.

2.3. Bulk organic geochemistry and optical analyses of Particulate Organic Matter

The main geochemical characteristics of particulate organic matter were defined with a Rock-Eval 6 pyrolyser (Vinci Technologies), which overcomes OM isolation by digestive processes ((HCl/HF attacks) of the mineral fractions. Basically, this thermal degradation method consists of a pyrolysis and followed by oxidation of the samples (details in Lafargue et al., 1998). The OC content (in wt. %, uncertainty 3 to 5%) is given by the sum of the POC calculated during the pyrolysis (Pyrolysed Carbon, PC) and oxidation (Residual Carbon, RC) steps.

Particulate Organic Matter (POM) was also characterized regarding its optical assemblage with quantitative palynofacies signatures (Graz et al., 2010) where each particle class is expressed in mg g^{-1}. After the isolation of the POM from the sample (2-5 g dried at 30°C) by acid digestion (HCl/HF) of the mineral fraction, the POM was then observed under light microscopy (Leica DMR XP) in transmitted light (objective x50) using a grid (10 μm mesh). In this analysis, 200 elementary surfaces were considered in order to obtain an error percentage lower than 5%. The classes of POM are defined on the basis of morphological, textural and colorimetric criteria (Tyson, 1995). The full optical quantitative results were published in Eyrolle et al. (2019). For this study, we focus either on greyish and gelified amorphous organic matter and gelified particles, characterizing the aquatic OM particles (POMa), and the opaque pyrogenic particles defined by some devolatilization vacuoles and their contribution to the total particulate assemblage (POMa and pyro ratio, table 1). In order to convert and keep the weighted contribution of POMa (α term in the equation 5) to the total optical assemblage of POM into the POCa contribution to the POC (section 3.5), and at first approximation, we hypothesize that the weighted contribution of C in OM remains broadly constant whatever the origins of POM.

2.4. Carbon 14 analyses

The radiocarbon contents were analyzed using an accelerator mass spectrometer. Sample preparation consisted of washing the sample (0.5 M HCl, 0.1 M NaOH) and then drying it under vacuum to eliminate carbonates. Samples were decarbonated to focus only on the organic counterpart. Decarbonated samples were then sealed in quartz tubes under vacuum with an excess of CuO and silver wire. Tubes were introduced into a furnace at 835°C for 5hr to convert the organic carbon into CO_2. The quartz tubes were then broken under vacuum to release, dry, measure, and collect the CO_2. The graphite target was obtained with a direct catalytic reduction of CO_2 using iron powder as a catalyst (Merck® for analysis reduced, 10 µm particles). The reduction reaction occurred at 600°C with excess H_2 (H_2/CO_2 = 2.5) and was complete after 4-5 hr. The iron-carbon powder was pressed into a flat pellet and stored under pure argon in a sealed tube. To reduce contamination from modern carbon or memory effects, all quartz and glass dishes were burned at 450°C for at least 5 hr. A turbo-molecular pump reaching 10^{-6} mbar was used to evacuate the vacuum lines. Measurements were performed using the Artemis facility (Moreau et al. 2013) with a 3 MV NEC Pelletron Accelerator coupled with a spectrometer dedicated to radiocarbon dating, measuring ^{12}C, ^{13}C and ^{14}C contents and counting the ^{14}C ions by isobaric discriminations. The analyses required 1 to 100 mg of dry sample (to obtain 1 mg of carbon). Riverine ^{14}C is commonly expressed as an enrichment factor ($\Delta^{14}C$ in ‰, eq. 1). $\Delta^{14}C$ integrates (i) the year of measurement (y), (ii) the average life of ^{14}C atom within a sample until it decays (tmean = 8267 y), (iii) the year for which the standard (i.e. oxalic acid I; OX-I) is decay-corrected (1950), (iv) the $^{14}C/^{12}C$ isotopic ratio of the sample (^{14}R) and (v) the $^{14}C/^{12}C$ isotopic ratio of the OX-I (^{14}Rs), readers can refer to Mook and van der Plicht, 1999 and Trumbore et al., 2016 for further details).

$$\Delta^{14}C\ (‰) = [^{14}R / (0.95 \,.\, ^{14}Rs \,.\, \exp(^{(y-1950)/8267)})-1] \,.\, 1000 \quad \text{(Eq. 1)}$$

The average standard deviation of $\Delta^{14}C$ is ± 3‰, and a positive value indicates a ^{14}C-enrichment from ^{14}C bomb and/or NPPs releases, a negative value indicates a ^{14}C dilution from various aged POC while ^{14}C-avoid compounds age over 60 ky reach -1000‰

(Trumbore et al., 2016). $\delta^{13}C$ expresses the enrichment or depletion of the ^{13}C stable isotope during physico-chemical or metabolic processes (e.g. photosynthesis) and is calculated as follow (eq. 2):

$$\delta^{13}C\ (‰) = [(^{13}R / {}^{13}R_{PDB})-1] \cdot 1000 \quad \text{(Eq. 2)}$$

In this equation 2, ^{13}R is the isotopic ratio $^{13}C/^{12}C$ of the sample and $^{13}R_{PDB}$ is that of the international standard (Pee Dee Belemnite, PDB, Smith and Epstein, 1971).

Practically, $\delta^{13}C$ signatures can be used to assess the contributions of various carbon sources transferred by rivers (Aucour et al., 1999). However, $\delta^{13}C$ signatures of aquatic plants can overlap with those of terrestrial materials (Raymond and Bauer, 2001). Accordingly, the combination of $\delta^{13}C$ and $\Delta^{14}C$ values used in this work (fig. 3 and 5) can help to better determine the C sources from recently fixed C to aged or petrogenic organic C stored in deep soil horizons and sedimentary rocks (Raymond et Bauer, 2001).

2.5. Petrogenic POC content assessment

Mean POCp values (wt. %) in sedimentary archives can be determined by plotting the sedimentary OC contents and the product of these values with the corresponding modern fraction (Fm) of the sample (Galy et al., 2008). Linear modelling provides the POCp content when the line defined by equation 3 crosses the x-axis. However, three criteria must be met prior to the use of this method (Galy et al., 2008): (i) the sedimentary OC in the samples should be seen as a binary mixture of petrogenic and biospheric POC (POCp, POCb), (ii) the POCp content should be almost constant within the sedimentary archive, and (iii) the mean radiocarbon content of POCb (i.e. Fmb) should also be relatively constant within the sedimentary archive. When these criteria are met, the data plotted in the diagram produce a linear trend.

$$OC \cdot Fm = OC \cdot Fmb - POCp \cdot Fmb \quad \text{(Eq 3)}$$

$$\text{when } OC.Fm = 0, \text{ then } OC = POCp$$

where OC (sedimentary OC) and POCp are expressed in wt. %, Fm is the measured radiocarbon composition of the sample (fraction of modern C) and Fmb is the radiocarbon composition of the POCb in the sample.

2.6. POCa content assessment and Freshwater Reservoir Effect (FRE)

The POCa content was assessed from the bulk organic geochemistry analyses coupled with the optical study of the quantitative palynofacies, as previously described in Eyrolle et al. (2019). During its growth, aquatic OM incorporates carbon from the dissolved inorganic load in rivers and thus, its ^{14}C content most generally reflects part of the dissolved inorganic ^{14}C contents ($DI^{14}C$) (Aucour et al., 1999). In turn, the $DI^{14}C$ contents mostly depends on the importance of weathering processes of sedimentary rocks (carbonate and, to a lesser extent, siliceous) in the catchment occurring on the surface and in groundwaters, delivering the inorganic dead-carbon dissolved load of rivers (Deevey et al., 1954). Despite exchanges of gaseous inorganic carbon that tend toward equilibrium between atmospheric and river systems, fossil DIC ages the river DIC and consequently the POCa. Hence, the FRE corresponds to the difference between the age of the freshwater carbon reservoirs and the age of the atmospheric carbon reservoirs (Ascough et al. 2010).

3. RESULTS AND DISCUSSION

3.1 $\Delta^{14}C$ and $\delta^{13}C$ signals of the riverine POC

At the studied station, the $\Delta^{14}C$ values in the sediment core ($\Delta^{14}C$-OC) exhibit a general increasing trend from the bottom to the surface and can be divided into 3 main periods (fig. 5, tab. 1). The 1923 to 1959 period is characterized by $\Delta^{14}C$ values ranging from -629 to -463 ‰, revealing a POC source that was either severely processed (pedogenesis, sediment cascade and/or POC spiraling) and/or either diluted by a POCp contribution. Although it may be an imprint of aerial aquatic plants, the $\delta^{13}C$ signature remains mostly inherited from C3 plants and/or type III kerogen since aquatic plants held labile C preferentially mineralized (fig. 6). The second period, from 1961 to 1986 exhibits two peaks in 1971 (-2 ‰) and in 1986

300 (236 ‰) with depleted $\Delta^{14}C$ value in 1978 (-105 ‰). The last period, from 1990 (176‰) to
301 2016 (222 ‰), shows weak $\Delta^{14}C$ variation. The POC sources for these two latter periods
302 were less subjected to these aging processes (particularly from 1961 to 1980) and broadly
303 exhibit a $\delta^{13}C$ signature of terrestrial C3 plants with a possible imprint of aerial aquatic plants
304 in samples showing positive $\Delta^{14}C$ values (fig. 6, tab. 1).
305 On the whole, and with the exception of the last period, and the peak in 1986, these $\Delta^{14}C$
306 values are systematically lower than those registered in the atmosphere over the same
307 periods of time. There are several explanations for the disequilibrium between the $\Delta^{14}C$
308 calculated from the OC of the riverine sediments and that from the atmosphere. Two of them
309 relate to the POC originating from the catchment: (i) a dilution effect by POCp and the part of
310 POCrw older than 60 ky, leading to reduced ^{14}C contents in sediments and decreased $\Delta^{14}C$
311 values and (ii) a gap between the ^{14}C activity in POCs and POCrw and that in the
312 atmosphere.
313 For the latter point and, as seen in the figure 5, these gaps can be positive or negative
314 depending on the age of OM stored in the soil profiles of the catchment or in the various
315 superficial deposits and the occurrence of erosion processes over time. Finally, another
316 explanation addresses the $\Delta^{14}C$ values specific to POCa stored in the sediments. Indeed, the
317 ^{14}C contents of this organic fraction can be expected to reflect several components
318 combining the ^{14}C released by nuclear industry, the local FRE and the equilibrium with the
319 atmosphere.
320 According to the $\delta^{13}C$ values, most of the organic matter stored in the sediments originates
321 from the C3 terrestrial plants and/or aerial aquatic plants (fig. 6). The shift of +2 ‰ of the $\delta^{13}C$
322 values with depth (fig. 6, tab. 1) may be attributed to a wide range of factors. Among them, a
323 possible minor changes in the source of the C3-plants, a change in the ratio POCs/POCa in
324 the sedimentary OC, and some microbial processes as seen for the lacustrine sediments
325 (Brenner et al., 1999) or for soil profiles (Torn et al., 2002). For the last factor, this

enrichment in 13C may be related to the enhanced metabolism of the lighter isotope, which may be promoted by microbes (e.g. Torn et al., 2002).

3.2. POCp content in the sedimentary archive

In figure 7 expressing the linear modelling, the results show two linear trends characterized by a correlation coefficient of over 0.95. The trend referring to the period from 1923 to 1959 indicates very low POCp content (0.01 wt. %) and the second referring to the period from 1961 to 2016, reveals a POCp amount of 0.59 wt%. Accordingly, the two groups of points evidenced in the previous section (1961-1986 and 1990-2016 periods) cannot be clearly identified and would have shown a very bad linear relation in the figure 7. This difference in POCp content over these two periods of time suggests a major change in sediment sources. One of the serious candidates for explaining this change in the beginning of the 1960s could originate from the land use management trends and the conversion of grassland into agricultural area. Indeed re-parcelling, which was marked by an increase in agricultural field size, provoked the near-eradication of hedges coupled with the digging of ditches. These surface processes, which are rooted in the global increase in demand for food production and yield, enhance drainage, reroute a part of the sediments in various reservoirs, and promote erosion and the transfer of new sedimentary sources within the catchment (Foucher et al, 2014). These changes are also the origin of the eutrophication of the Loire River, as evidenced by the increase in authigenic calcite and phosphorous concentrations in a previously studied twin core (Grosbois et al., 2012). Hence, it is reasonable to hypothesize that the POCs, POCrw and POCp could have had a different origin starting in 1961, but no argument can be further advanced at this point to precisely determine the source of this petrogenic counterpart. At first glance, and based on the POCp content close to 0.60 wt.%, the source could be some OC/clay-rich sedimentary rocks, such as marls or schists, with a higher OC content than the other main sedimentary rocks (Ronov and Yaroshevski, 1976,

353 Copard et al., 2007). Such sedimentary rocks from the Mesozoic Age (Lias) outcrop along
354 the Middle Loire River and are a part of Paris Basin.
355
356 **3.3. $\Delta^{14}C$ signal of POCb over the last decades**
357 By using the POCp/OC ratio (tab. 1), the $\Delta^{14}C$ values of POCb, including that of both aquatic
358 (POCa) and terrestrial organic carbon (POCs+POCrw), can be calculated (fig. 5) by using
359 equation (4):
360 $$\Delta^{14}C\text{-}POCb = \Delta^{14}C\text{-}OC / (1 - POCp/OC) \quad \text{(Eq. 4)}$$
361 with OC and POCp expressed in wt. %, $\Delta^{14}C$-POC as the calculated values of the sediment
362 samples, and $\Delta^{14}C$-POCb as the theoretical $\Delta^{14}C$ values of biospheric POC.
363
364 While the first previously identified period (1923 to 1959) exhibits no change, as expected
365 ($\Delta^{14}C$-POCb = $\Delta^{14}C$-OC), due to the low amounts of POCp, the second period (1961 to 2016)
366 shows theoretical $\Delta^{14}C$-POCb values (from 12 to 368 ‰) higher than the $\Delta^{14}C$-OC ones
367 (from -193 to 222 ‰). These results overall highlight that POCp may significantly dilute the
368 ^{14}C content measured in riverine sediments and in sedimentary archives.
369
370 **3.4. $\Delta^{14}C$-POCa over the last decades**
371 Among all the OC components that compose riverine sedimentary archives, POCa is the
372 single component that can be expected to provide evidence for ^{14}C liquid discharge from the
373 nuclear industry. Over the period 1961-2010, the POCa content, assimilated to the OMa
374 ratio, within the studied sedimentary archive showed a low contribution to the total optical
375 assemblage of POM (8% as a mean value, tab. 1). Low amounts of POCa are generally
376 expected in most riverine sedimentary archives since these compounds, which are enriched
377 in lipids, are preferentially degraded during early processes (Burdige, 2007). These results
378 suggest that riverine sedimentary archives cannot be expected to store or reveal the ^{14}C
379 releases from the nuclear industry performed over years. Nevertheless, to subtract this POC

component from the POCb signal, we estimated the Δ^{14}C-POCa by using additional data sets acquired from radiological monitoring and survey (SYRACUSE IRSN database).

Before the beginning of nuclear energy production by NPPs (PWR) in 1980 (fig. 1, Dampierre NPPs) and assuming the absence of ^{14}C nuclear releases before this period of time, the Δ^{14}C-POCa values would express a part of the FRE. Thus, the age given by FRE was required in order to estimate the DI^{14}C content of the Loire River upstream NPPs. Even though FRE depends on hydrological conditions and tributary inputs, involving a large range of FRE values, we used a mean FRE value of 1194±30 ^{14}C yr (Coularis et al., 2016), i.e. approximately -143 ‰. This mean FRE value characterizes the upper part of the Loire basin and overcomes the potential influence of NPPs. To assert whether the nuclear releases were recorded in aquatic plants, we used the radiocarbon data from some aquatic mosses (n= 21) collected upstream and downstream of the Belleville-sur-Loire NPPs as these mosses do not exhibit aerial surfaces that promote $^{14}C_{atm}$ fixation during photosynthesis. The Mean Δ^{14}C values of aquatic mosses collected in 1999 and 2000 upstream and downstream of the Belleville-sur-Loire NPPs reached -164, and -176 ‰ respectively, while the $\Delta^{14}C_{atm}$ ranged from 121 to 115 ‰. With respect to the uncertainties associated with FRE, these data show that aquatic mosses in the Loire River are generally in equilibrium with the FRE. Importantly, these data show that the measured mosses do not record the ^{14}C liquid releases from nuclear activities. However, this statement should be considered with caution due to (i) the deficiency of the representativeness of the samples for radiocarbon measurement purposes and (ii) the ^{14}C plume from the nuclear releases, which depends on the local hydrodynamic conditions, remains unknown. For the latter reason, we can hypothesize that if the sampling of aquatic plants are outside the plume, there is obviously no ^{14}C imprint from the NPPs. Finally, a mean value of -10 ‰ C for Δ^{14}C-POCa was extracted from the IRSN radiocarbon data and corresponds to the ^{14}C activity measured for the mosses and also for aerial aquatic plants such as *Carex* (n= 13) and *Phalaris* (n=8) growing along the riverbank.

3.5. Reconstruction of $\Delta^{14}C$-POCt over the last decades

By using the POMa contribution (α □□□□□□□□□□□□□□□□□□□□□□□□the □O□□ contribution to the sedimentary OC, see section 2.3) to the total optical assemblage of POM acquired over the period 1961-2010 with the quantitative palynofacies method (Eyrolle et al., 2019), the $\Delta^{14}C$-POCt can be obtained by using the equation (5):

$$\Delta^{14}C\text{-POCt} = \Delta^{14}C\text{-POCb} - (\alpha.\Delta^{14}C\text{-POCa})/(1-\alpha) \qquad \text{(Eq. 5)}$$

As expected, the $\Delta^{14}C$-POCt values are generally lower than that of POCb (fig. 5, tab. 1). These results finally underline that the ^{14}C contents characterizing the terrestrial POC is far from the atmospheric referential value over the whole period covered by the sedimentary archive. As POCt consists of a mixture of POCs and recent POCrw (stored in the catchment as superficial formations), the gaps can be explained since (i) it is well known that POCs shows a large range of ^{14}C contents with depth (e.g. Schmidt et al., 2011, Trumbore, 2009) and (ii) superficial formations, such as old riverine deposits (terraces) or colluviums, can also hold a wide range of OM younger than 60 kyr (e.g. Brown et al., 2009). In other words, the $\Delta^{14}C$-POCt values routed by rivers clearly depend on the portion of soil depth and that of the recent sediment, which are both being mobilized by erosion processes. As previously described, the profile can be divided into three main distinct periods:

From 1923 to 1959, since is there neither petrogenic (POCp = 0.01 wt.%) nor aquatic contributions to the ^{14}C content of sedimentary OM, the $\Delta^{14}C$-POCt signal fit well with that of the $\Delta^{14}C$ calculated for the sediment. However, the substantial gap between the $\Delta^{14}C$-POCt and $\Delta^{14}Catm$ values corresponds to a mean age of 6247±847 14C years for POCt deposited in the sedimentary sink, which is far older than that given for the bulk sediment with the age model (Grosbois et al. 2012; Eyrolle et al;, 2019). This involves that erosion processes occurring in the catchment have mobilized essentially highly aged POCt over this period of time. Such POC could be held either by Holocene detrital riverine deposits in the basin, and/or deep soil horizons showing a low turnover of soil organic carbon (Schmidt et al., 2011).

From 1959 to 1986 and as seen in the figure 5, at the beginning of the 1960s, a major shift toward higher values occurs for Δ^{14}C-POCt (from -463 to -39 ‰). This shift was also enhanced by the occurrence of petrogenic OM (fig. 7, POCp = 0.59 wt.%). In 1969 (Δ^{14}C-POCt = 385 ‰), another shift decreased the Δ^{14}C until 1978 (Δ^{14}C-POCt = 136 ‰) and then it increased until 1986 (Δ^{14}C-POCt = 508 ‰). The 1969 shift is due to the beginning of atmospheric fallout from nuclear tests; however a time lag of 5 to 7 years was observed in the sedimentary archive. This time lag is interpreted as the mean transit time from the source of sediments in the catchment to the sedimentary sink in the river system. The subsequent decrease in 1969 is concomitant with the occurrence of carbonized organic particles, likely depleted in ^{14}C content, with vacuole devolatilization as charcoals (fig. 8). This suggests either a significant fire event or an industrial incident along the Loire corridor. These particles supply the sedimentary compartment up to 1975. Afterward, the steady increase in Δ^{14}C-POCt until 1986 may reflect the residence time of the system, almost 20 years, for such particles.

From 1986 to 2010, the Δ^{14}C-POCt values steadily decreased from 508 to 139 ‰ while the Δ^{14}Catm values in the atmosphere decreased from 197 to 22 ‰ for the same period of time. The mean gap between Δ^{14}C-POCt and Δ^{14}Catm reaches 212±65 ‰ over this period of time. This is consistent with the works of Levin and Heishaimer (2000) indicating that the terrestrial biospheric reservoir is a source of ^{14}C for the atmosphere at least since the end of 1980s.

3.6. Transit time of POCt from the catchment to the river sediments

Based on our dataset, the transit time of the OM route in the catchment can be assessed by comparing the Δ^{14}C peak level in the atmosphere in 1963 with the Δ^{14}C-POCt peak in the sedimentary archives. Indeed, the terrestrial OM has previously fixed atmospheric ^{14}C during its growth on the catchment following photosynthesis (e.g. Schurr et al., 2016) prior its route toward the deposition area and its burial in river sediments. As a consequence, this POCt has only kept in memory the atmospheric ^{14}C during its growth. Since there is no additional 14C incorporation in OM after its death, a mean transit time can be estimated by comparing

462 the time lag between the well know $\Delta^{14}C$ peak level in the atmosphere in 1963 with that
463 preserved within the sedimentary OC (fig. 5). This latter peak may have occurred over the
464 period 1970-1985. The fire event occurring in 1969 prevents any accurate determination of
465 its date. Nonetheless, a minimum and maximum transit time for POCt of 7 and 22 years,
466 referring to the time lags from 1963 to 1970 and 1985, respectively, can be estimated for the
467 Loire basin. Such time lags are in agreement with our previous estimation of 5-7 years made
468 at the beginning 1960s (see above) as those provided by using organically bound tritium
469 (Eyrolle et al., 2019).
470

471 **4. CONCLUSIONS AND PERSPECTIVES**

472 We aim to decipher the $\Delta^{14}C$-OC values in sediments from one of the most nuclearized rivers
473 in Europe. For a similar period and as expected, the ^{14}C levels in these materials are far
474 different from those in the atmosphere. There are several reasons for this discrepancy. The
475 first is the dilution of the radiocarbon contents by dead-carbon inherited from the erosion of
476 outcropping sedimentary rocks and aged superficial formations in the catchment. The
477 proportion of the dead-carbon can be easily determined with a linear modelling. Due to the
478 combination of previously published optical measurements, a mean FRE value and a
479 radiocarbon dataset for aquatic organic matter sampled along the river corridor, the
480 contribution of aquatic POC to the $\Delta^{14}C$-OC was also calculated. The $\Delta^{14}C$-POCa reflects the
481 FRE and not the ^{14}C liquid discharge from the nuclear industry. Hence, both the terrestrial
482 (i.e. soils and younger superficial formations) contribution to the $\Delta^{14}C$ of the riverine and
483 sedimentary OC and the age of these terrestrial OM could be easily assessed. Despite our
484 inability to split the respective contribution of the soil and the superficial formations to the ^{14}C
485 content of terrestrial organic matter, the $\Delta^{14}C$ signature of riverine OC could be refined into
486 three parts. In this respect, such a method of $\Delta^{14}C$ reconstruction would also be a powerful
487 tool for defining the transit time of sediments in a river. For example, in the Loire River, the
488 transit time could be between 7 and 22 years, however future studies are required to validate
489 this tool. This radiocarbon unravelling could also point to the milestones of the social and

economic trajectories for a considered catchment and their consequence for sediment and C dynamics in rivers. Here, some major changes in land use, caused by re-parcelling, were identified during the 1960s; these changes, in turn, triggered a reroute of the sediments in the river bringing in some new sedimentary organic matter. The age of terrestrial OM before and after the 1960s clearly indicates the rejuvenation of POCt stored in sediments, suggesting a major change in sedimentary sources in the catchment. In addition, coupled with the palynofacies method of characterizing the particulate organic assemblage, ^{14}C unravelling is suitable for identifying events that occurred in the catchment, such as an industrial accident or a fire event. Here, these events impacted both the radiocarbon concentration of terrestrial POC and the optical assemblage in the river sediments during the end of the 1960s. The incursion of these specific particles depleted in radiocarbon was observed up to 1986, suggesting that the resilience of the riverine system to this event is almost 20 years. Last, the gap between $\Delta^{14}C_{atm}$ and that of the terrestrial POC clearly shows that the terrestrial biospheric reservoir is a source term of ^{14}C for the atmosphere since at least 1986.

Acknowledgments

This work was funded by the Institute for Radioprotection and Nuclear Safety (IRSN-NEEDS, project PALYNO) and a part of the TRAJECTOIRE project from the French National Research Agency (ANR-19-CE3-0009, 2020-2024). Warm thanks are addressed to J.P Bakyono, F. Giner, D. Mourier and C. Le Corre for their precious help during field sampling, sample preparation and sample analyses. The authors also sincerely thank the three anonymous reviewers and the editor for their appreciated help in the improvement the manuscript.

References

518 Ascough, P. L., Cook, G. T., Church, M. J., Dunbar, E., Einarsson, A., Mc Govern, T. H.,
519 Gugmore, A. J., Perdikaris, S., Hastie, H., Fridriksson, A. & Gestsdottir, H. (2010).
520 Temporal and spatial variations in freshwater 14C reservoir effects: Lake Mývatn, northern
521 Iceland. *Radiocarbon, 52*(2–3), 1098–112. https://doi.org/10.1017/S003382220004618X
522 Aucour, A. M., Sheppard, S. M. F., Guyomar, O. & Wattelet, J. (1999). Use of 13C to trace
523 origin and cycling of inorganic carbon in the Rhone river system. *Chemical Geology,*
524 *159*(1-4), 87–105. https://doi.org/10.1016/S0009-2541(99)00035-2
525 Bauer, J. E., Druffel, E. R. M., Wolgast, D.M., & Griffin, S. (2001). Sources and cycling of
526 dissolved and particulate organic radiocarbon in the northwest Atlantic continental margin.
527 *Gobal Biogeochemical Cycles, 15*(3), 615-636. https://doi.org/10.1029/2000GB001314
528 Berndt, C., Frenzel, P., Ciner, A., Ertunc, G., & Yildirim, C. (2019). Holocene marginal marine
529 ostracod successions from Kizilirmak River delta; implications for depositional
530 environments and sea-level changes at the Southern Black Sea coast. *Sedimentary*
531 *Geology, 382*, 103-121. https:///doi.org/10.1016/j.sedgeo.2019.01.013
532 Brenner, M., Whitmore, T. J., Curtis, J. H., Hodell, D. A., & Schelske, C. L. (1999). Stable
533 isotope ($\delta^{13}C$, $\delta^{15}N$) signatures of sedimented organic matter as indicators of historic lake
534 trophic state. *Journal of Paleolimnology*, *22*, 205-221, https://doi:
535 10.1023/A:1008078222806
536 Brown, A. G., Carey, C., Erkens, G., Fuchs, M., Hoffmann, T., Macaire, J. J., Moldenhauer,
537 K. M., & Walling, D. E. (2009). From sedimentary records to sediment budgets: Multiple
538 approaches to catchment sediment flux. *Geomorphology, 108,* 35–47,
539 http://doi:10.1016/j.geomorph.2008.01.021
540 Brugeron, A., Schomburgk, S., Cabaret, O., Bault, V., Bel, A., Salquerbe, D. & Fourniguet, G.
541 Lamotte, C. & Parmentier, M. (2018). Synthèse sur la cartographier et la caractérisation
542 des alluvions dans le referentiel hydrogéologique BDLISA depuis sa version 1. Rapport
543 final. BRGM/RP67533-FR, 193p.
544 Burdige, D.J. (2007). Preservation of organic matter in marine sediments: controls,
545 mechanisms and imbalance in sediment organic carbon budgets? *Chemical Reviews,*

546 *107*(2), 467-485. https://doi.org/10.1021/cr050347q
547 Cathalot, C., Rabouille, C., Tisnerat-Laborde, N., Toussaint, F., Kerhervé, P., Buscail, R.,
548 Loftis, K., Sun, M., Tronczynski, J., Azoury, S., Lansard, B., Treignier, C., Pasto,r L., &
549 Tesi, T. (2013). The fate of river organic carbon in coastal areas: a study in the Rhône
550 River delta using multiple isotopic ($\delta^{13}C$, $\Delta^{14}C$) and organic tracers. *Geochimica*
551 *Cosmochimica Acta, 118*(1), 33–55. https://doi.org/10.1016/j.gca.2013.05.001
552 Cerling, T. E., Harris, J. M., MacFadden, B. J., Leakey, M. G., Quade, J., Eisenmann, V., &
553 Ehleringer, J. R. (1993). Global vegetation change through the Miocene/Pliocene
554 boundary. *Nature, 389*, 153-158. https://doi.org/10.1038/38229
555 Chappuis, E., Seriñá, V., Martí, E., Ballesteros, E., & Gacia, E. (2017). Decrypting stable-
556 isotope ($\delta^{13}C$ and $\delta^{15}N$) variability in aquatic plants. *Freshwater Biology, 62*(11), 1907-
557 1818. https://doi.org/10.1111/fwb.12996
558 Copard, Y., Amiotte-Suchet, P., & Di-Giovanni, C. (2007). Storage and release of fossil
559 organic carbon related to weathering of sedimentary rocks. *Earth and Planetary Science*
560 *Letters, 258*, 345-357. https//doi:10.1016/j.epsl.2007.03.048
561 Copard, Y., Eyrolle, F., Radakovitch, O., Poirel, A., Raimbault, P., Gairoard, S., & Di-
562 Giovanni, C. (2018). Badlands as a hot spot of petrogenic contribution to riverine
563 particulate organic carbon to the Gulf of Lion (NW Mediterranean Sea). *Earth Surface*
564 *Processes and Landforms, 43*(12), 2495-2509, https://doi.org/10.1002/esp.4409
565 Coularis, C., Tisnérat-Laborde, N., Pastor, L., Siclet, F., & Fontugne, M. (2016). Temporal
566 and spatial variations of freshwater reservoir ages in the Loire River watershed.
567 *Radiocarbon, 58*(3), 549-56. https//doi:10.1017/RDC.2016.36
568 Deevey, E. S. J., Gross, M. S., Hutchinson, G. E., & Kraybill, H. L. (1954). The natural C14
569 contents of materials from hard-water lakes. *Proceedings of the National Acadamy of*
570 *Sciences of the USA, 40*, 285–288. https://doi.org/10.1073/pnas.40.5.285
571 Dezileau, L., Terrier, B., Berger, J. F., Blanchemanche, P., Latapie, A., Freydier, R.,
572 Bremond, L., Paquier, A., Lang, M., & Delgado, J. L. (2014). A multidating approach

applied to historical slackwater flood deposits of the Gardon River, SE France. *Geomorphology, 214*, 56-68. https//doi.org/10.1016/j.geomorph.2014.03.017

Eyrolle, F., Copard, Y., Lepage, H., Ducros, L., Morereau, A., Grosbois, C., Cossonnet, C., Gurriaran, R., Booth, S., & Desmet, M. (2019). Evidence for tritium persistence as organically bound forms in river sediments since the past nuclear weapon tests. *Scientific Reports, 9*, 11487. http//doi.org/10.1038/s41598-019-47821-1

Foucher, A., Salvador-Blanes, S., Evrard, O., Simonneau, A., Chapron, E., Courp, T., Cerdan, O., Lefèvre, I., Adriaensen, H., Lecompte, F., & Desmet, M. (2014). Increase in soil erosion after agricultural intensification: Evidence from a lowland basin in France. *Anthropocene, 7*, 30-41. https://doi.org/10.1016/j.ancene.2015.02.001

Galy, V., Beyssac, O., France-Lanord, C., & Eglinton, T.I. (2008). Recycling of graphite during Himalayan erosion: a geological stabilization of carbon in the crust. *Science, 322*, 943–945. http//doi:10.1126/science.1161408

Fryirs, K.A., Brierley, G., Preston, N. J., & Kasai, M. (2007). Buffers, barriers and blankets: the (dis)connectivity of catchment-scale sediment cascades. *Catena*, *70*, 49-67. https://doi.org/10.1016/j.catena.2006.07.007

Gavin, D. G. (2001). Estimation of inbuilt age in radiocarbon ages of soil charcoal for fire history studies. *Radiocarbon, 43*, 27–44. https://doi.org/10.1017/S003382220003160X

Graven, H., Allison, C. E., Etheridge, D. M., Hammer, S., Keeling, R. F., Levin, I., Meijer, H. A. J., Rubino, M., Tans, P. P., Trudinger, C. M., Vaughn, B. H., & White, J. W. C. (2017). Compiled records of carbon isotopes in atmospheric CO2 for historical simulations in CMIP6. *Geoscientific Model Development, 10*, 4405-4417. https//doi.org/10.5194/gmd-10-4405-2017

Graz, Y., Di-Giovanni, C., Copard, Y., Laggoun-Défarge, F., Boussafir, M., Lallier-Vergès, E., Baillif, P., Perdereau, L., & Simonneau, A. (2010). Quantitative palynofacies analysis as a new tool to study transferts of fossil organic matter in recent terrestrial environments. *International Journal of Coal Geology, 84*, 49–62. https//doi:10.1016/j.coal.2010.08.006

Grosbois, C., Meybeck, M., Lestel, L., Lefevre, I., & Moatar, F. (2012). Severe and contrasted polymetallic contamination patterns (1900- 2009) in the Loire River sediments (France). *Science of the Total Environment, 435–436*, 290–305. https://doi.org/10.1016/j.scitotenv.2012.06.056

Hedges, J. I., Keil, R. G., & Benner, R. (1997). What happens to organic matter in the ocean? *Organic Geochemistry, 27*(5–6), 195–212. https://doi.org/10.1016/S0146-6380(97)00066-1

Kohn, M.J. (2010). Carbon isotope compositions of terrestrial C3 plants as indicators of (paleo) ecology and (paleo) climate. *Proceedings of the National Academy of Sciences USA, 107*, 19691–19695. https://doi.org/10.1073/pnas.1004933107

Lafargue, E., Marquis, F., & Pillot, D. (1998). Rock-Eval 6 applications in hydrocarbons exploration, production and soil contamination studies. *Revue de l'Institut Français du Pétrole, 53*(4), 421-437. https://doi.org/10.2516/ogst:1998036

Leithold, E. L., Blair, N. E., & Perkey, D. W. (2006). Geomorphic controls on the age of particulate organic carbon from small mountainous and upland rivers. *Global Biogeochemical Cycles, 20*(3), https://doi.org/10.1029/2005GB002677

Levin, I., & Hesshaimer, V. (2000). Radiocarbon – a unique tracer of global carbon cycle dynamics. *Radiocarbon, 42*(1), 69-80. https://doi.org/10.1017/S0033822200053066

MacDonald, G. M., Beukens, R. P., Kieser, W. E., & Vitt, D. H. (1987). Comparative radiocarbon dating of terrestrial plant macrofossils and aquatic moss from the "ice-free corridor" of western Canada. *Geology*, 15, 837-840.

Marwick, T. R., Tamooh, F., Teodoru, C. R., Borges, A. V., Darchambeau, F., & Bouillon, S. (2015). The age of river-transported carbon: a global perspective. *Global Biogeochemical Cycles, 29*, 122–137, https//doi:10.1002/2014GB004911

Meybeck, M. (2006). Origins and behaviours of carbon species in world rivers. *In*: Roose, J., et al. (Eds.), *Soil Erosion and Carbon Dynamics*, pp. 209–238 (chapter 15).

Mook, W. G., & van der Plicht, J. (1999). Reporting radiocarbon activites and concentrations. *Radiocarbon, 41*, 227–2239. https://doi.org/10.1017/S0033822200057106

628 Moreau, C., Caffy, I., Comby-Zerbino, C., Delqué-Količ, E., Dumoulin, J. P., Hain, S., Quiles,
629 A., Setti, V., Souprayen, C., Thellier, B., & Vincent, J. (2013). Research and development
630 of the ARTEMIS 14C AMS facility : Status report. *Radiocarbon, 55*, 331–337.
631 https://doi.org/10.1017/S0033822200057441
632 Naegler, T., & Levin, I. (2009). Biosphere-atmosphere gross carbon exchange flux and the
633 d13CO2 and D14CO2 disequilibria constrained by the biospheric excess radiocarbon
634 inventory. *Journal of Geophysical Research - Atmosphere,*
635 *114*(D17). https://doi.org/10.1029/2008JD011116
636 Newbold, J. D., Mulholland, P. J., Elwood, J. W., O'Neill, R. V. (1982). Organic carbon
637 spiralling in stream ecosystems. *Oikos, 38*, 266-272.
638 O'Leary, M. H. (1988). Carbon isotopes in photosynthesis. *BioScience, 38*(5), 328-336. DOI:
639 10.2307/1310735
640 Oswald, W. W., Anderson, P. M., Brown, T. A., Brubaker, L. B., Hu, F. S., Lozhkin, A. V.,
641 Tinner, W., &Kaltenrieder, P. (2005). Effects of sample mass and macrofossil type on
642 radiocarbon dating of arctic and boreal lake sediments. *The Holocene, 15*, 758–767.
643 https://doi.org/10.1191/0959683605hl849rr
644 Raymond, P. A., & Bauer, J. E. (2001). Use of 14C and 13C natural abundances for
645 evaluating riverine, estuarine, and coastal DOC and POC sources and cycling: A review
646 and synthesis. *Organic Geochemistry, 32*(4), 469–485. https://doi.org/10.1016/S0146-
647 6380(00)00190-X
648 Raymond, P. A., Hartmann, J., Lauerwarld, R., Sobek, S., McDonald, C., Hoover, M.,
649 Butman, D., Striegl, R., Mayorga, E., Humborg, C., Kortelainen, P., Dürr, H., Meybeck, M.,
650 Ciais, P., & Guth, P. (2013). Global carbon dioxide emissions from inland waters. *Nature,*
651 *503*, 355-359. https//doi:10.1038/nature12760
652 Ronov, A. B., & Yaroshevsky, A. A. (1976). A new model for the chemical structure of the
653 Earth crust. *Geochemistry International, 13*, 89-121.

654 Rumpel, C., Kögel-Knabner, I., & Bruhn, F. (2002). Vertical distribution, age, and chemical
655 composition of organic carbon in two forest soils of different pedogenesis. *Organic*
656 *Geochemistry, 33*(10), 1131–1142. https://doi.org/10.1016/S0146-6380(02)00088-8
657 Schmidt, M. W. I., Torn, M. S., Abiven, S., Dittmar, T., Guggenberger, G., Janssens, I. A.,
658 Kleber, M., Kögel-Knabner, I., Lehmann, J., Manning, D. A. C., Nannipieri, P., Rasse, D.
659 P., Weiner, S., & Trumbore, S.E. (2011). Persistence of soil organic matter as an
660 ecosystem property. *Nature, 478*, 49-56. https//doi:10.1038/nature10386
661 Schurr, E. A. G., Carbone, M. S., Hicks Pries, C. E., Hopkins, F. M., & Natali, S. M. (2016).
662 Radiocarbon in terrestrial systems. In E. A. G. Schuur, E. R. M. Druffel, & S. E. Trumbore
663 (Eds.), Radiocarbon and Climate Change, Mechanisms, Applications and Laboratory
664 Techniques (pp. 167–220). Springer International Publishing
665 Smith, B. N., & Epstein, S. (1971). Two categories of C-13/C-12 ratios for higher plants. *Plant*
666 *Physiology, 47*, 380-381. https//doi:10.1104/pp.47.3.380
667 Soon, W., Baliunas, S. L., Robinson, A. B., & Robinson, Z.W. (1999). Environmental effect of
668 increased atmospheric carbon dioxide. *Climatic Research, 13*(2), 149–164.
669 https://doi.org/10.1260/0958305991499694
670 Stuiver, M., & Polach, H. A. (1977). Reporting of 14C data. *Radiocarbon, 19*, 355–363.
671 http//doi.org/10.1016/j.forsciint.2010.11.013
672 Sundquist, E. T. (1993). The global carbon dioxide budget. *Science, 259*(5097), 934–941.
673 DOI: 10.1126/science.259.5097.934
674 Torn, M. S., Lapenis, A. G., Timofeev, A., Fischer, M. L., Babikov, B. V., & Harden, J. W.
675 (2002). Organic carbon and carbon isotopes in modern and 100-year-old-soil archives of the
676 Russian steppe. *Global Change Biology, 8*, 941-953. https//doi:10.1111/j.1365-
677 2486.2005.00916.x
678 Trumbore, S. E. (2009). Radiocarbon and soil carbon dynamics. *Annual. Review of Earth*
679 *and Planetary Sciences, 37*, 47-66. https//doi: 10.1146/annurev.earth.36.031207.124300
680 Trumbore, S. E., Sierra, C. A., & Hick Pries, C. E. (2016). Radiocarbon Nomenclature,
681 Theory, Models, and Interpretation: Measuring Age, determining cycling rates, and

682 Tracing Source Roles. In E. A. G. Schuur, E. R. M. Druffel, & S. E. Trumbore (Eds.),
683 Radiocarbon and Climate Change, Mechanisms, Applications and Laboratory Techniques
684 (pp. 45–82). Springer International Publishing.
685 Tyson, R.V. (1995). Sedimentary Organic Matter: Organic Facies and Palynofacies.
686 Chapman and Hall, London. (615 pp.).
687 Walling, D. E. (1983). The sediment delivery problem. *Journal of Hydrology, 65*, 209-237.
688 https://doi.org/10.1016/0022-1694(83)90217-2
689 Wang, X., Xu, C., Druffel, E. R. M., Xue, Y., & Qi, Y. (2016). Two black carbon pools
690 transported by the Changjiang and Huanghe Rivers in China. *Gobal Biogeochemical*
691 *Cycles, 30*, 1778–1790. https//doi:10.1002/2016GB005509
692 Zhou, A., He, Y., Wu, D., Zhang, X., Zhang, C., Liu, Z., & Yu, J. (2015). Changes in the
693 radiocarbon reservoir age in lake Xingyun, Southwestern China during the Holocene.
694 *PLoS ONE*, 10(3): e0121532. doi:10.1371/journal.pone.0121532
695
696 SYRACUSE database: www.irsn.fr/FR/expertise/rapports_expertise/surveillance-
697 environnement/Pages/Bilan-etat-radiologique-environnement-France-2015-2017.aspx
698

699 **Figures caption**

700 Figure 1: *study site showing the coring site and the spatial distribution of nuclear power*
701 *plants along the Loire River (France), and its main contributors (from Eyrolle et al., 2019).*
702 *Nuclear technologies are indicated as UNGG (natural uranium, graphite and gaz) and PWR*
703 *(Pressurized water reactors) with their respective period of use.*

704

705 Figure 2: *(A): core sedimentary log showing the main lithology, (B): particle size distribution*
706 *and mean diameter D50 (µm), (C): activities of radiocesium (Bq* kg^{-1}*) and Pu ratio (x1000)*
707 *signals leading to the age model. The two peaks of* ^{137}Cs *in 1963 (due to peak emissions*
708 *from nuclear weapons tests in the atmosphere), then in 1986 (due to atmospheric fallout*
709 *from the Chernobyl accident in Europe), and the two peaks of* $^{238}Pu/^{239+240}Pu$ *activity ratio in*
710 *1969 and 1980 (occurring after the Saint-Laurent-des-Eaux nuclear reactor accidents) were*
711 *used as chronological references (from Eyrolle et al., 2019). Uncertainties on years are*
712 *estimated to be ±2 years. For A, B and C, the bottom core was fixed at 125 cm in order to*
713 *homogenise the beginning of these signals.*

714

715 Figure 3: *conceptual view of various particulate organic carbon (POC) sources in a*
716 *catchment (from the Bleone river system, upstream Digne les Bains, Alpes de Haute*
717 *Provence, France). POCa: aquatic POC as the autochthonous POC for the river system.*
718 *POCp (petrogenic POC), POCs (soil POC), POCrw (reworked POC), both considered as*
719 *allochtonous and respectively originating from: outcropping rocks, soils, superficial*
720 *formations. the two color codes for POCrw correspond to POC older (grey) and younger*
721 *(sepia) than 60 ky BP. Red circle correspond to a theoritical coring site containing*
722 *sedimentary OC. POCa, POCs and POCrw correspond to the biospheric POC (POCb) while*
723 *POCt includes POCs and POCrw. See also section 2.2 for details. (picture from Goolge*
724 *earth).*

725

Figure 4: *$\Delta^{14}C$ and $\delta^{13}C$ signatures of the main sources of riverine POC (adapted from Marwick et al., 2015). Atmospheric $\delta^{13}C$ and $\Delta^{14}C$ from atmospheric CO_2 (Graven et al., 2017), C3 plants: $\delta^{13}C$ (Kohn et al., 2010, O'Leary, 1988), – C4 plants $\delta^{13}C$ (Cerling et al., 1997), $\Delta^{14}C$ for C3 and C4 plants are in equilibrium with the atmosphere (e.g. Trumbore, 2009) - Aquatic plant: $\delta^{13}C$ for submerged and aerial plants (Chappuis et al., 2017), $\Delta^{14}C$ (SYRACUSE IRSN database) – $\delta^{13}C$ of kerogen (Tyson, 1995) (fossil OM, Tyson, 1995) is divided into three main type of organic matter: the type III encompasses all the terrestrial higher plants origin while the type I and II combine the lacustrine/bacterial and marine origins. Upward arrow corresponds to a possible contamination in ^{14}C either by ^{14}C gas or liquid releases by nuclear activities. A combination of C3-C4 plants can occurs in soils (mixing), pedogenesis in soils strictly involves POCs, sedimentary cascade in the catchment involves all the terrestrial POC (POCrw POCs) including POCp while POC spiralling in streams afflicts all the POC sources.*

Figure 5: *$\Delta^{14}C$ signals of the atmosphere reservoir and measured $\Delta^{14}C$ at the most downstream fluvial station of the Loire river basin of sedimentary OC (black circle); green diamond: rebuilt $\Delta^{14}C$ of biospheric POC (POCb), red diamond: rebuilt $\Delta^{14}C$ of terrestrial POC (POCt=POCs+POCrw) from the catchment.*

Figure 6: $\Delta^{14}C$ and $\delta^{13}C$ signatures of sedimentary OC stored in the Loire River. Samples are ranged in the aged and reworked or C3 / aerial aquatic plants POC signatures. While samples in black circles (belong to period 1923-1959) appear depleted in ^{14}C, these samples do not hold dead-C but rather show an aged POCs or POCrw signature. To the opposite, those in red circles (belong to the period 1961-2016) show a significant POCp contribution despite their high $\Delta^{14}C$ values, suggesting a significant enrichment in ^{14}C due to the atmospheric source. See also the legend of the figure 4 for further detailed explanations.

Figure 7: *linear modelling (from Galy et al., 2008) applied to the sediment samples. Red diamonds correspond to the period 1961-2016 (POCp = 0.59 wt.%) while the red one to the 1923-1959 period (POCp = 0.01 wt.%).*

Figure 8: *sedimentary pyrogenic ratio signal with time. The pyrogenic particle identified with the palynofacies method consists in opaque and corroded particle showing devolatilization vacuoles (Graz et al., 2010). If the background level of these particles is less than 1% of the total organic particles throughout the sedimentary core, a short period of time (1969-1976) is characterised by higher ratio suggesting a fire (natural or industrial) event with a resident time of 7 years.*

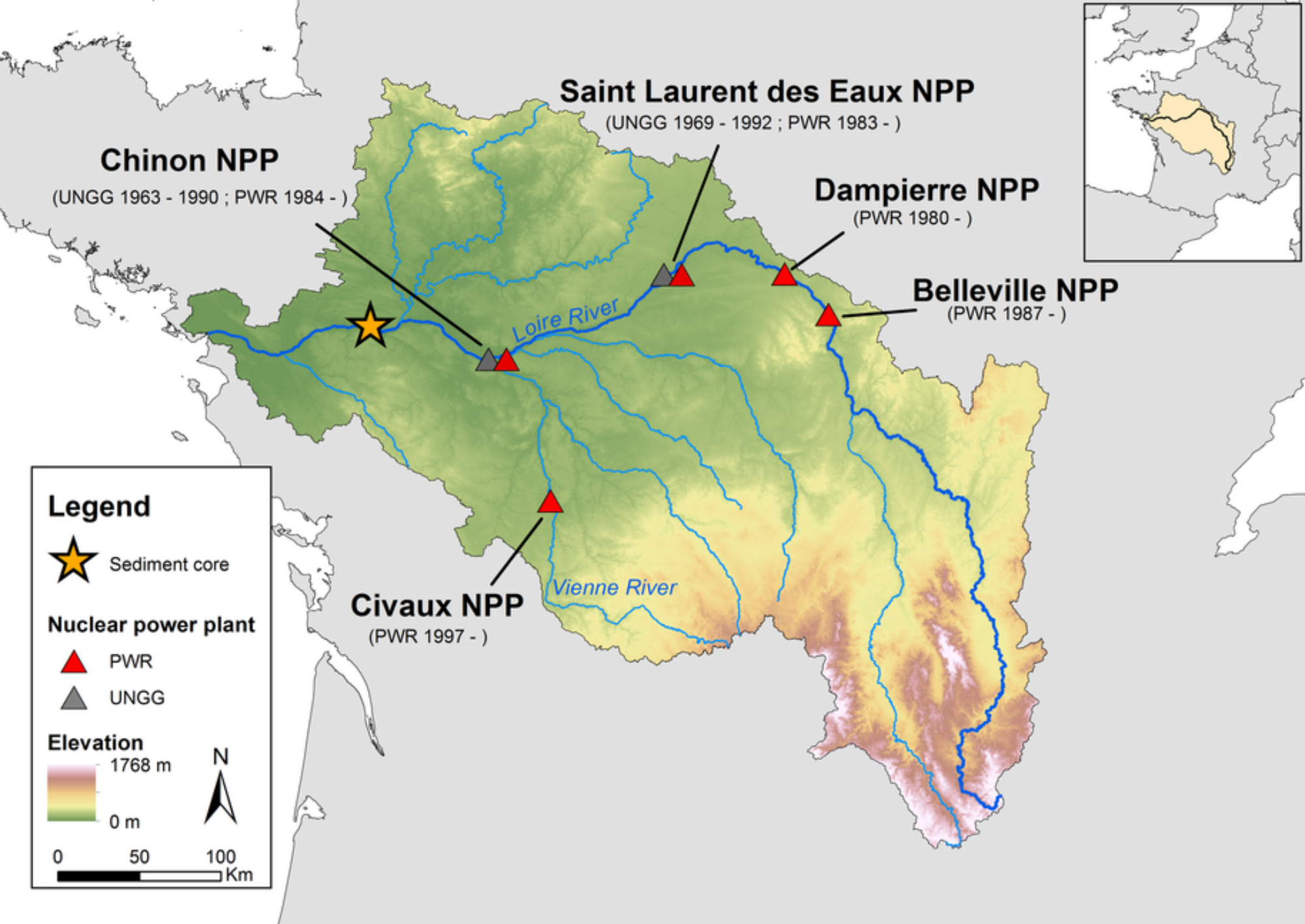
Saint Laurent des Eaux NPP
(UNGG 1969 - 1992 ; PWR 1983 -)
Chinon NPP
(UNGG 1963 - 1990 ; PWR 1984 -)
Dampierre NPP
(PWR 1980 -)
Belleville NPP
(PWR 1987 -)
Loire River
Vienne River
Civaux NPP
(PWR 1997 -)
Legend
Sediment core
Nuclear power plant
PWR
UNGG
Elevation
1768 m
0 m
N
0
50
100
Km

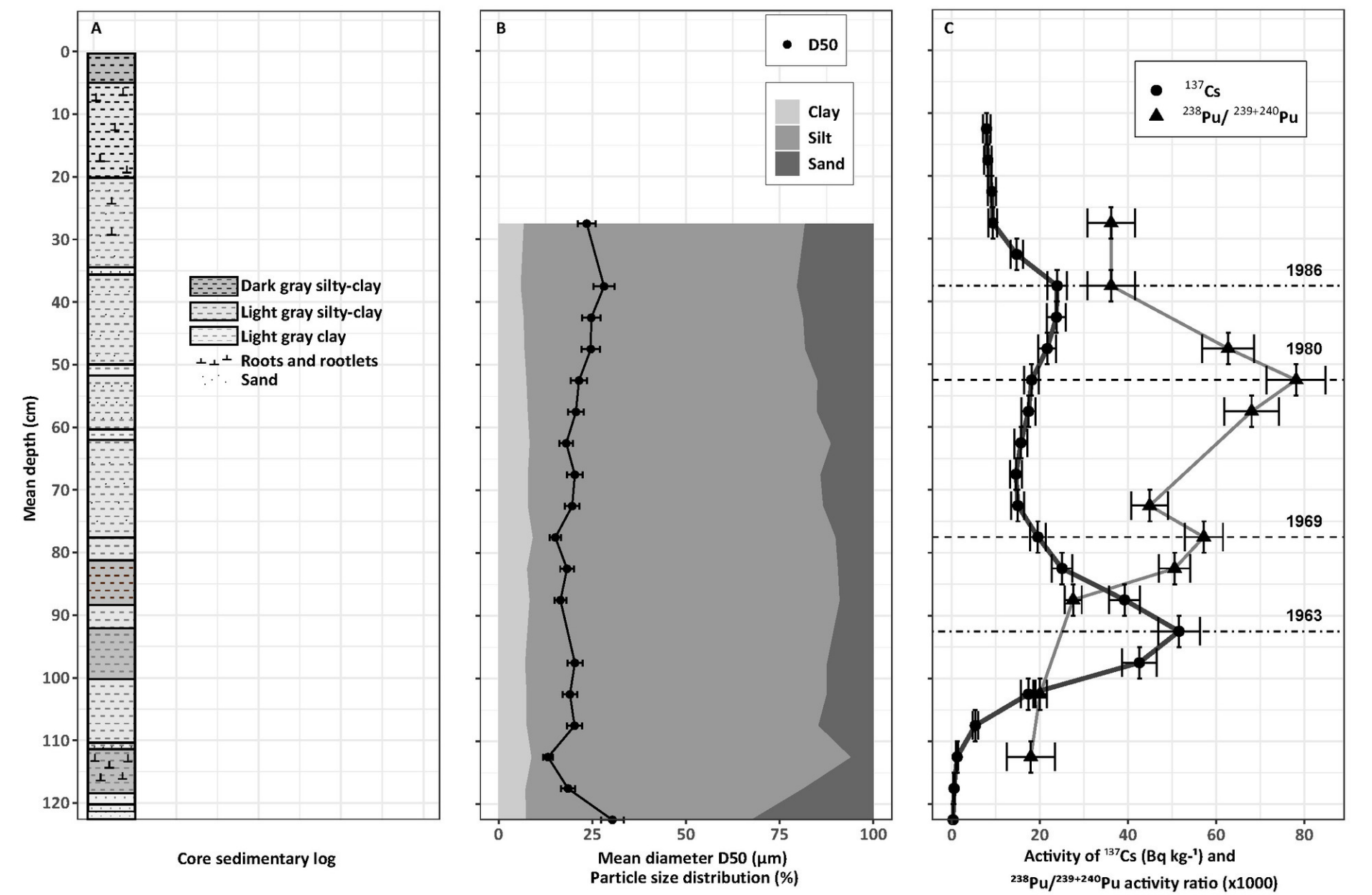
A
B
C
Mean depth (cm)
0
10
20
30
40
50
60
70
80
90
100
110
120
Dark gray silty-clay
Light gray silty-clay
Light gray clay
Roots and rootlets
Sand
Core sedimentary log
D50
Clay
Silt
Sand
0
25
50
75
100
Mean diameter D50 (µm)
Particle size distribution (%)
137Cs
238Pu/ 239+240Pu
1986
1980
1969
1963
0
20
40
60
80
Activity of 137Cs (Bq kg-1) and
238Pu/239+240Pu activity ratio (x1000)

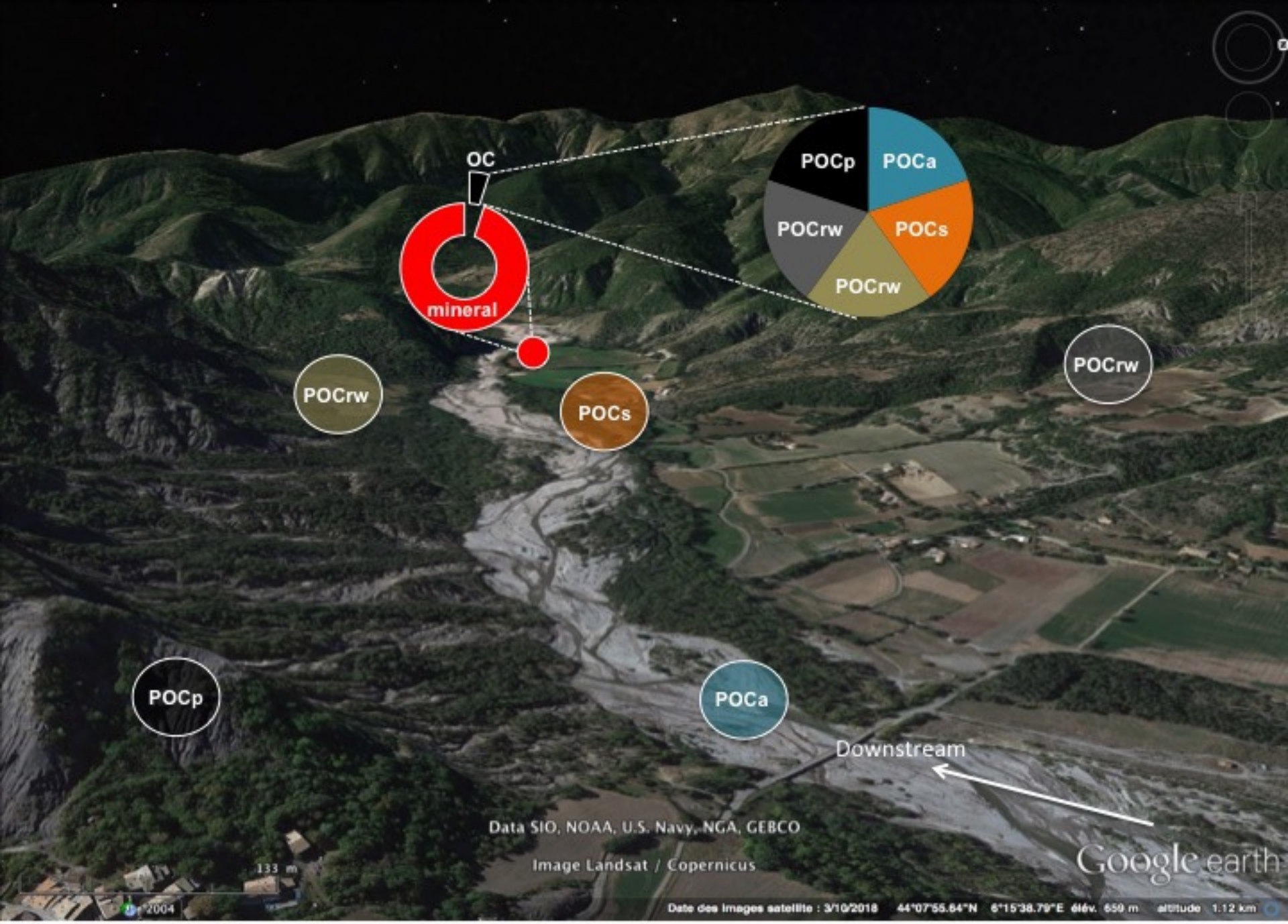
OC
mineral
POCp
POCa
POCrw
POCs
POCrw
POCrw
POCs
POCrw
POCp
POCa
Downstream
Data SIO, NOAA, U.S. Navy, NGA, GEBCO
Image Landsat / Copernicus
Google earth
133 m
2004
Date des images satellite : 3/10/2018
44°07'55.84"N
6°15'38.79"E
élév. 659 m
altitude 1.12 km

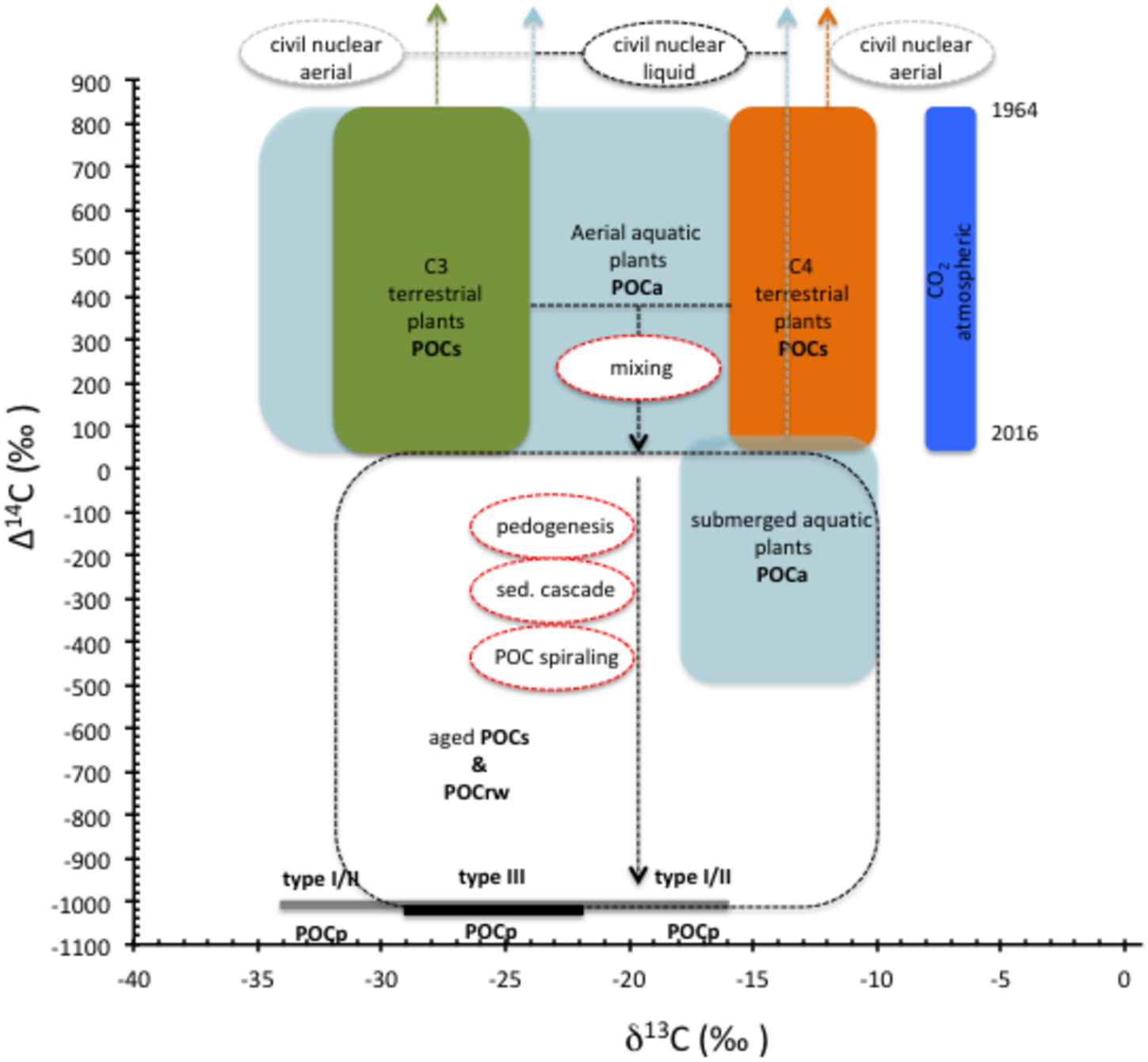
civil nuclear aerial
civil nuclear liquid
civil nuclear aerial
1964
2016
C3 terrestrial plants POCs
Aerial aquatic plants POCa
C4 terrestrial plants POCs
CO_2 atmospheric
mixing
pedogenesis
sed. cascade
POC spiraling
submerged aquatic plants POCa
aged POCs & POCrw
type I/II
type III
type I/II
POCp
POCp
POCp
$\Delta^{14}C$ (‰)
$\delta^{13}C$ (‰)
900
800
700
600
500
400
300
200
100
0
-100
-200
-300
-400
-500
-600
-700
-800
-900
-1000
-1100
-40
-35
-30
-25
-20
-15
-10
-5
0

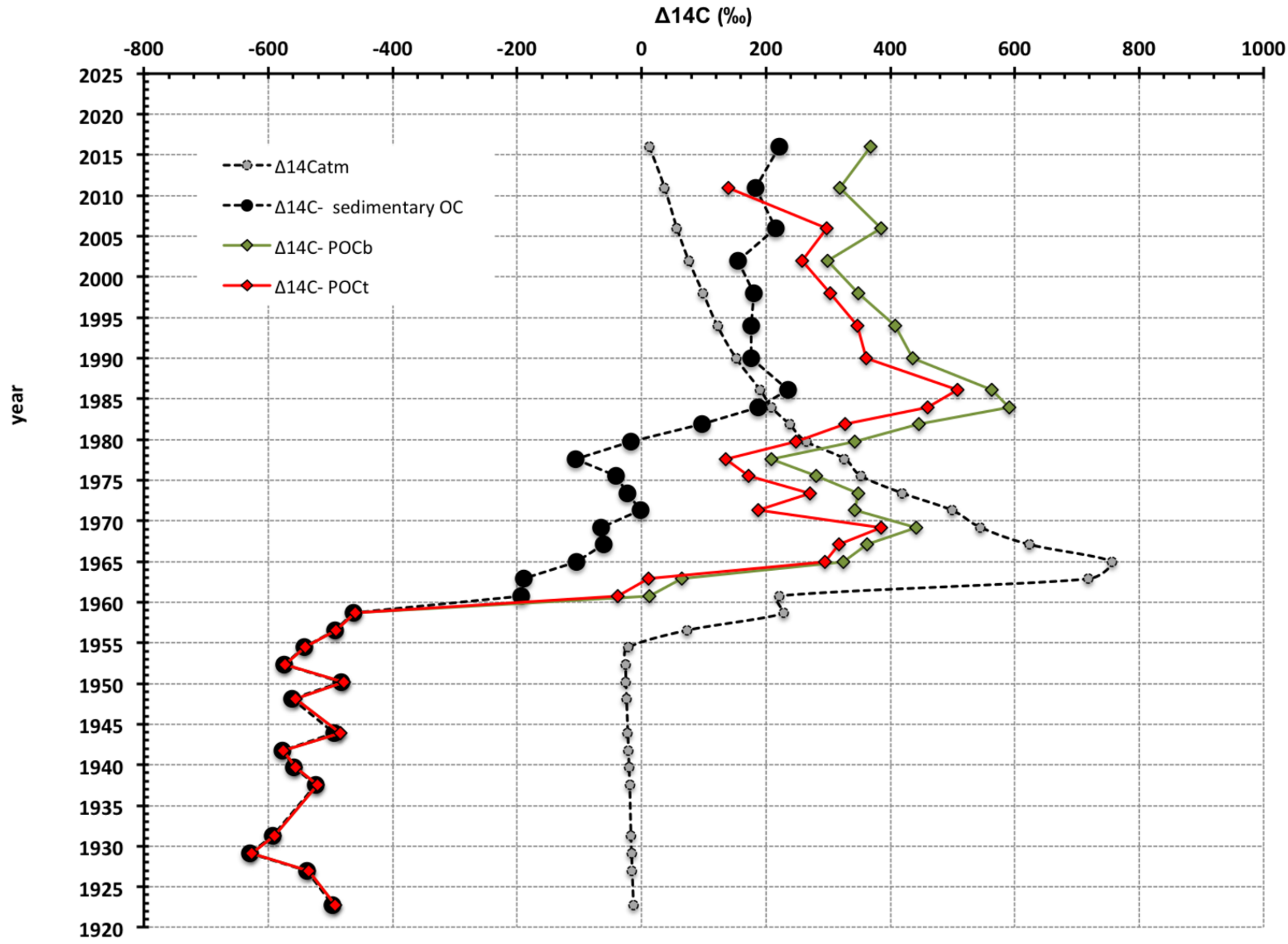
Δ14C (‰)
-800
-600
-400
-200
0
200
400
600
800
1000
year
2025
2020
2015
2010
2005
2000
1995
1990
1985
1980
1975
1970
1965
1960
1955
1950
1945
1940
1935
1930
1925
1920
Δ14Catm
Δ14C- sedimentary OC
Δ14C- POCb
Δ14C- POCt

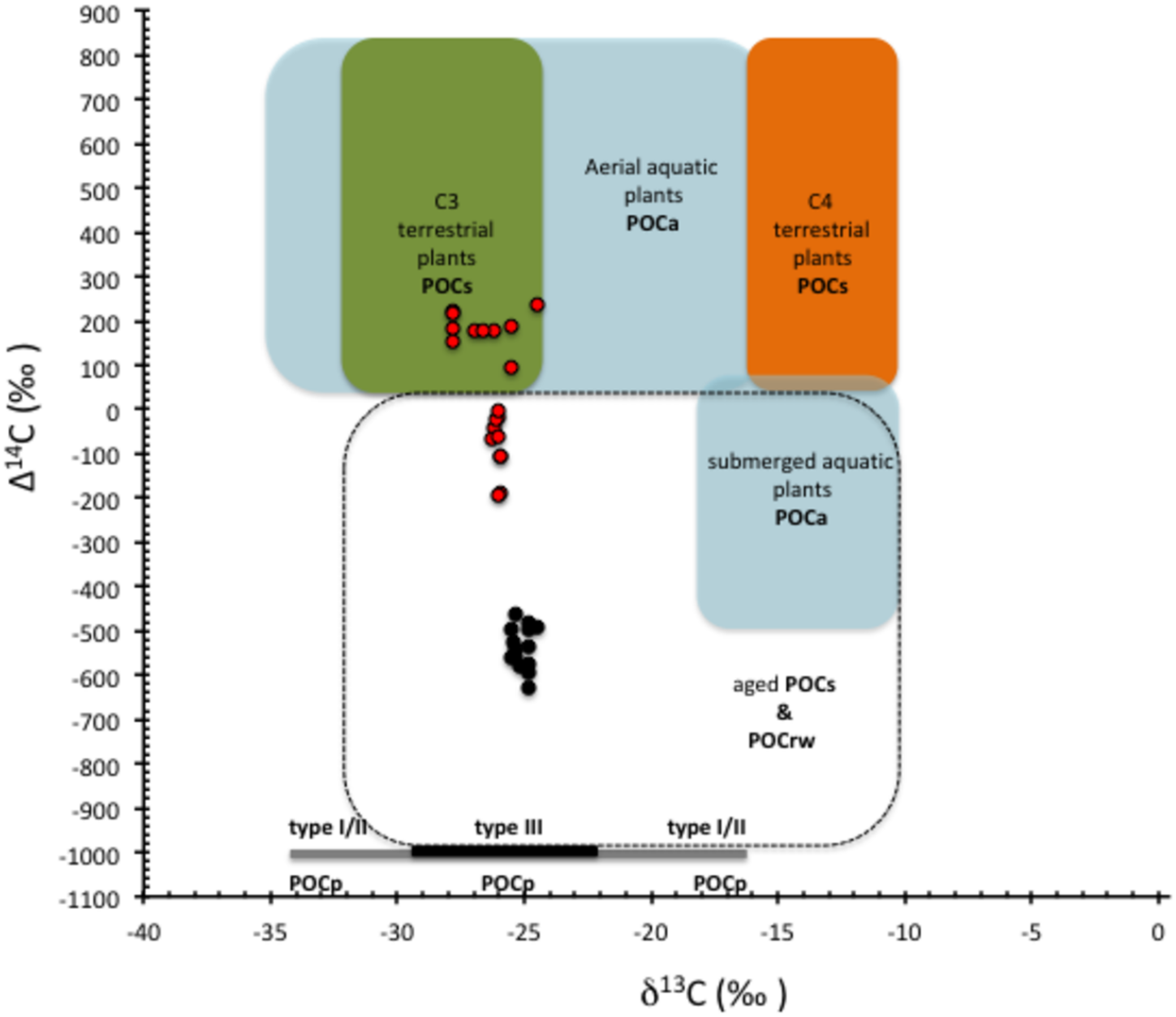
C3 terrestrial plants POCs
Aerial aquatic plants POCa
C4 terrestrial plants POCs
submerged aquatic plants POCa
aged POCs & POCrw
type I/II
type III
type I/II
POCp
POCp
POCp
Δ14C (‰)
δ13C (‰)
900
800
700
600
500
400
300
200
100
0
-100
-200
-300
-400
-500
-600
-700
-800
-900
-1000
-1100
-40
-35
-30
-25
-20
-15
-10
-5
0

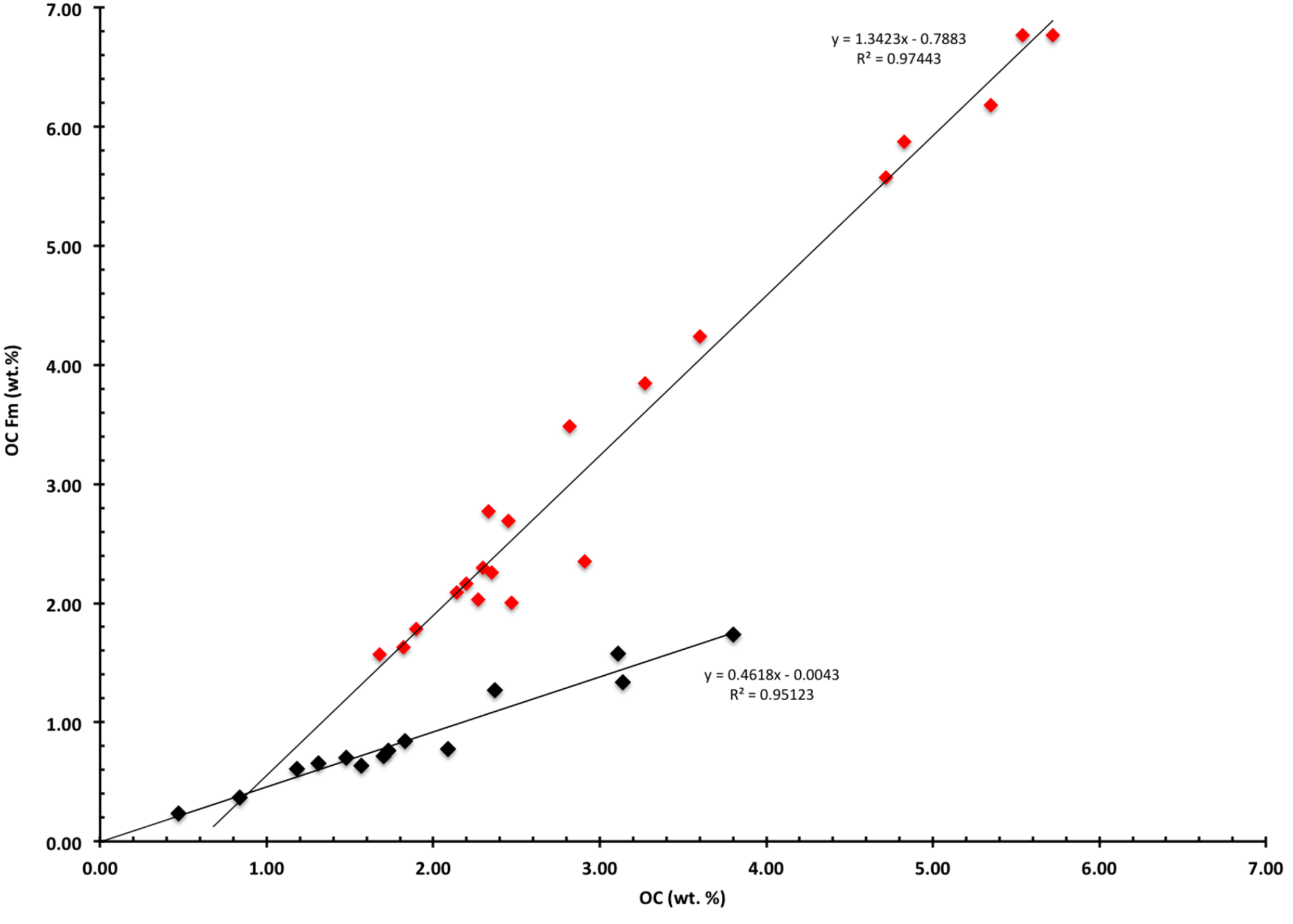
y = 1.3423x - 0.7883
R² = 0.97443
y = 0.4618x - 0.0043
R² = 0.95123
OC Fm (wt.%)
OC (wt. %)
0.00
1.00
2.00
3.00
4.00
5.00
6.00
7.00

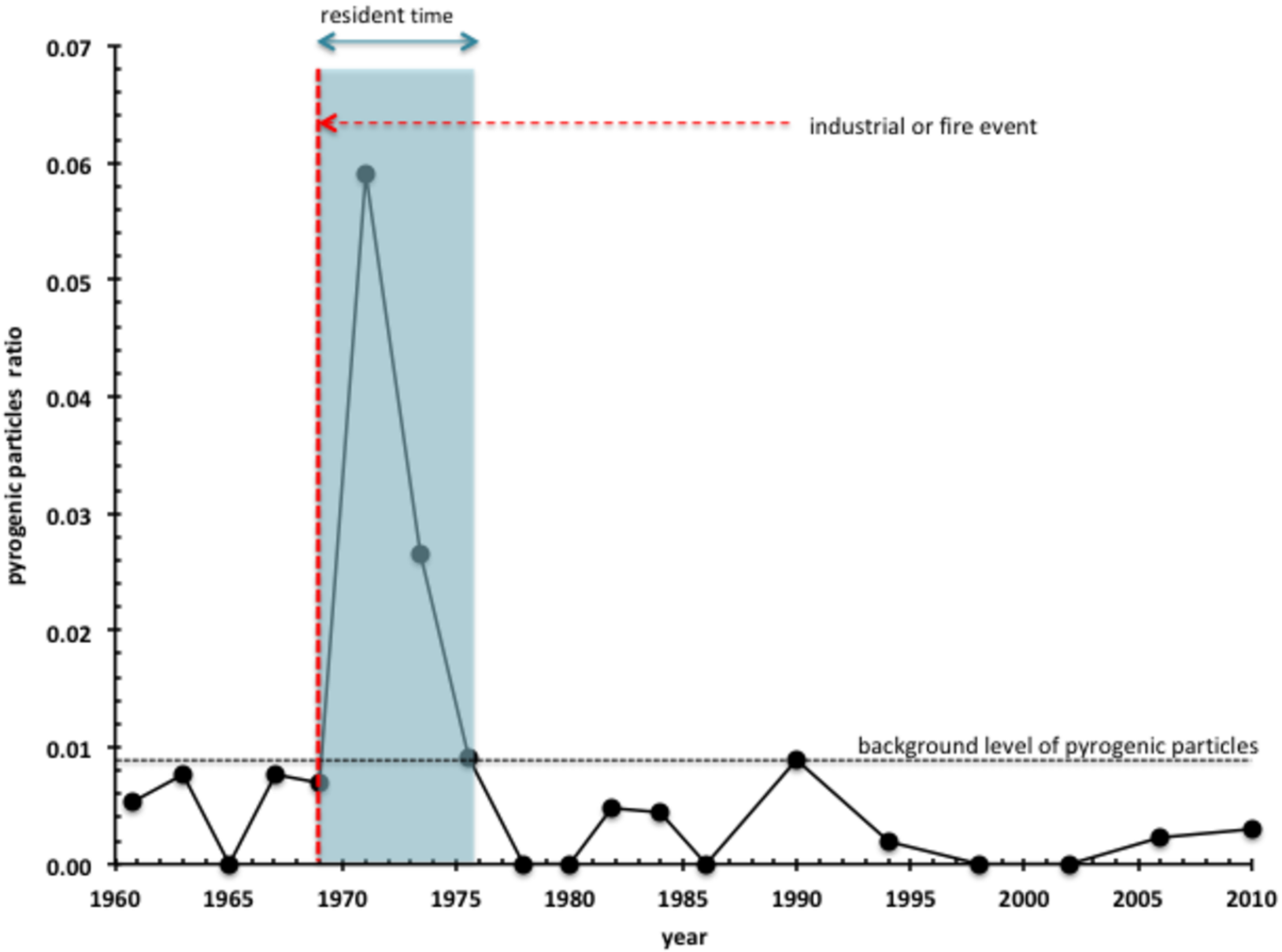
resident time
industrial or fire event
background level of pyrogenic particles
pyrogenic particles ratio
0.07
0.06
0.05
0.04
0.03
0.02
0.01
0.00
1960
1965
1970
1975
1980
1985
1990
1995
2000
2005
2010
year

table 1*: values of the main isotopic parameters of the riverine samples and that of the atmosphere ($\Delta^{14}C_{atm}$, Graven et al. 2017). Ages of the samples are calculated with an uncertainty of +/- 2 years from some isotopic methods ($^{238}Pu/^{239+240}Pu$ and ^{137}Cs, see Eyrolle et al., 2019). POMa and Pyro are two ratios corresponding respectively to the aquatic and the carbonized particles contributions to the total optical assemblage of OM given by the palynofacies method (Graz et al., 2010, see Eyrolle et al., 2019 for details). Fm corresponds to the fraction of modern as described in Mook and Van der Plitch (1999), POCp content is defined in the section 3.2 and in the equation 1. Little available sediment for the period 1923-1959 and 2016 explains the absence of optical results.*

depth (cm)	age	$\Delta^{14}C_{atm}$ (‰)	$\Delta^{14}C$-POC (‰)	$\delta^{13}C$ (‰)	Fm	POC (wt.%)	POCp/POC	$\Delta^{14}C$-POCb (‰)	$\Delta^{14}C$-POCt (‰)	POMa	Pyro
2.5	2016	13	222	-27.8	1.22	5.54	0.106	368	N/A	N/A	N/A
7.5	2011	37	183	-27.8	1.18	5.72	0.103	319	139	0.15	0.003
12.5	2006	57	216	-27.8	1.22	4.83	0.122	385	298	0.08	0.002
17.5	2002	76	156	-27.8	1.16	5.35	0.110	299	258	0.04	0.000
22.5	1998	99	180	-27	1.18	4.72	0.125	349	304	0.04	0.000
27.5	1994	122	177	-26.2	1.18	3.60	0.164	408	347	0.06	0.002
32.5	1990	152	176	-26.6	1.18	3.27	0.180	436	362	0.07	0.009
37.5	1986	191	236	-24.5	1.24	2.82	0.209	563	508	0.05	0.000
42.5	1984	209	188	-25.5	1.19	2.33	0.253	591	460	0.12	0.004
47.5	1982	238	97	-25.5	1.10	2.45	0.241	446	327	0.11	0.005
52.5	1980	265	-17	-26	0.98	2.20	0.268	343	248	0.09	0.000
57.5	1978	326	-105	-25.9	0.89	2.27	0.260	209	136	0.07	0.000
62.5	1976	353	-41	-26.2	0.96	2.35	0.251	281	172	0.10	0.009
67.5	1973	419	-23	-26.1	0.98	2.14	0.276	349	271	0.07	0.026
72.5	1971	499	-2	-26	1.00	2.30	0.257	342	187	0.13	0.059
77.5	1969	545	-64	-26.3	0.94	1.68	0.351	442	385	0.05	0.007
82.5	1967	624	-61	-26	0.94	1.90	0.311	363	318	0.04	0.008
87.5	1965	756	-105	-25.9	0.90	1.82	0.324	325	295	0.03	0.000
92.5	1963	718	-190	-25.9	0.81	2.47	0.239	64	12	0.05	0.008
97.5	1961	221	-193	-26	0.81	2.91	0.203	12	-39	0.05	0.005
102.5	1959	228	-463	-25.3	0.54	2.37	0.004	-461	-461	N/A	N/A
107.5	1957	73	-493	-24.5	0.51	3.11	0.003	-491	-491	N/A	N/A
112.5	1954	-21	-543	-25.3	0.46	3.80	0.003	-541	-541	N/A	N/A
117.5	1952	-25	-575	-24.8	0.43	3.14	0.003	-573	-573	N/A	N/A
122.5	1950	-25	-482	-24.8	0.52	1.18	0.008	-478	-478	N/A	N/A
127.5	1948	-24	-562	-25.3	0.44	0.84	0.012	-556	-556	N/A	N/A
137.5	1944	-22	-495	-25.5	0.50	0.47	0.021	-484	-484	N/A	N/A
142.5	1942	-21	-578	-25.2	0.42	1.70	0.006	-576	-576	N/A	N/A
147.5	1940	-20	-559	-25.5	0.44	1.73	0.006	-556	-556	N/A	N/A
152.5	1938	-19	-523	-25.4	0.48	1.48	0.007	-520	-520	N/A	N/A
167.5	1931	-17	-592	-24.8	0.41	1.57	0.006	-590	-590	N/A	N/A
172.5	1929	-16	-629	-24.8	0.37	2.09	0.005	-627	-627	N/A	N/A

177.5	1927	-15	-537	-24.8	0.46	1.83	0.005	-535	-535	N/A	N/A
187.5	1923	-13	-497	-24.8	0.50	1.31	0.008	-493	-493	N/A	N/A

Particulate Organic Carbon (POC) in riverine sedimentary archives

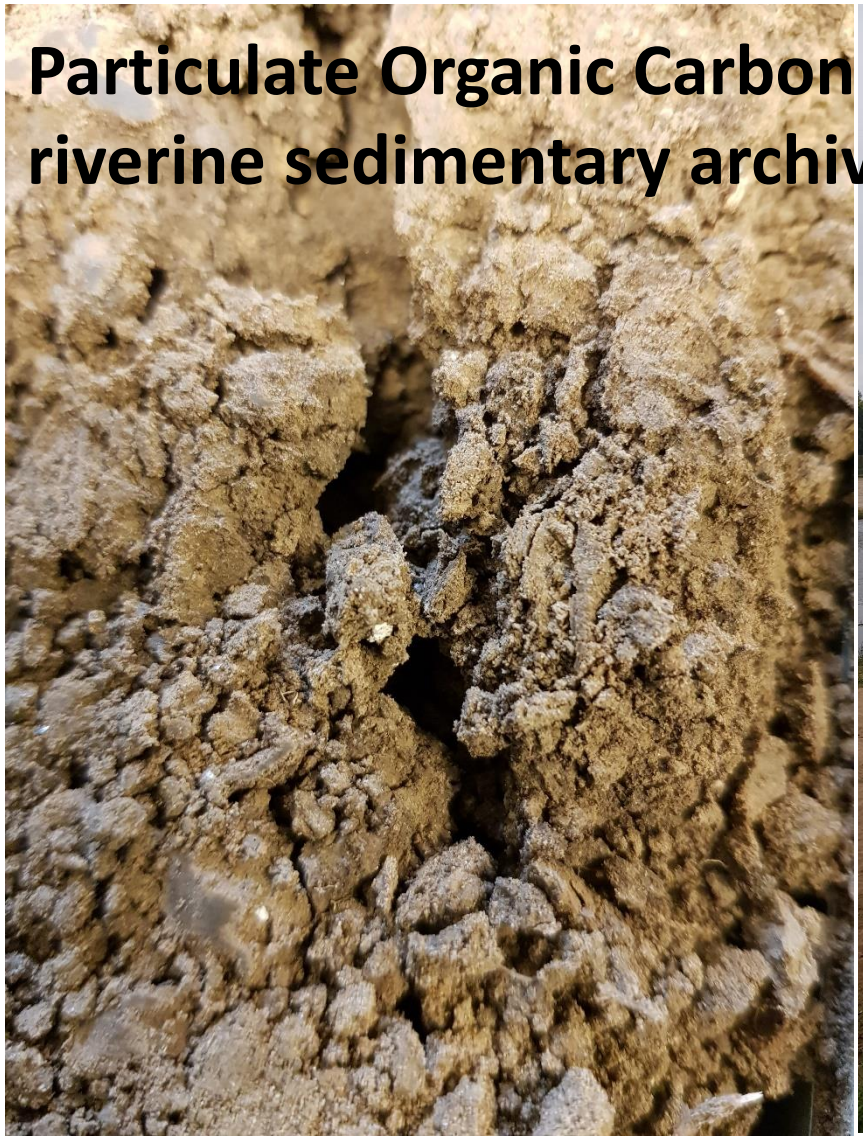

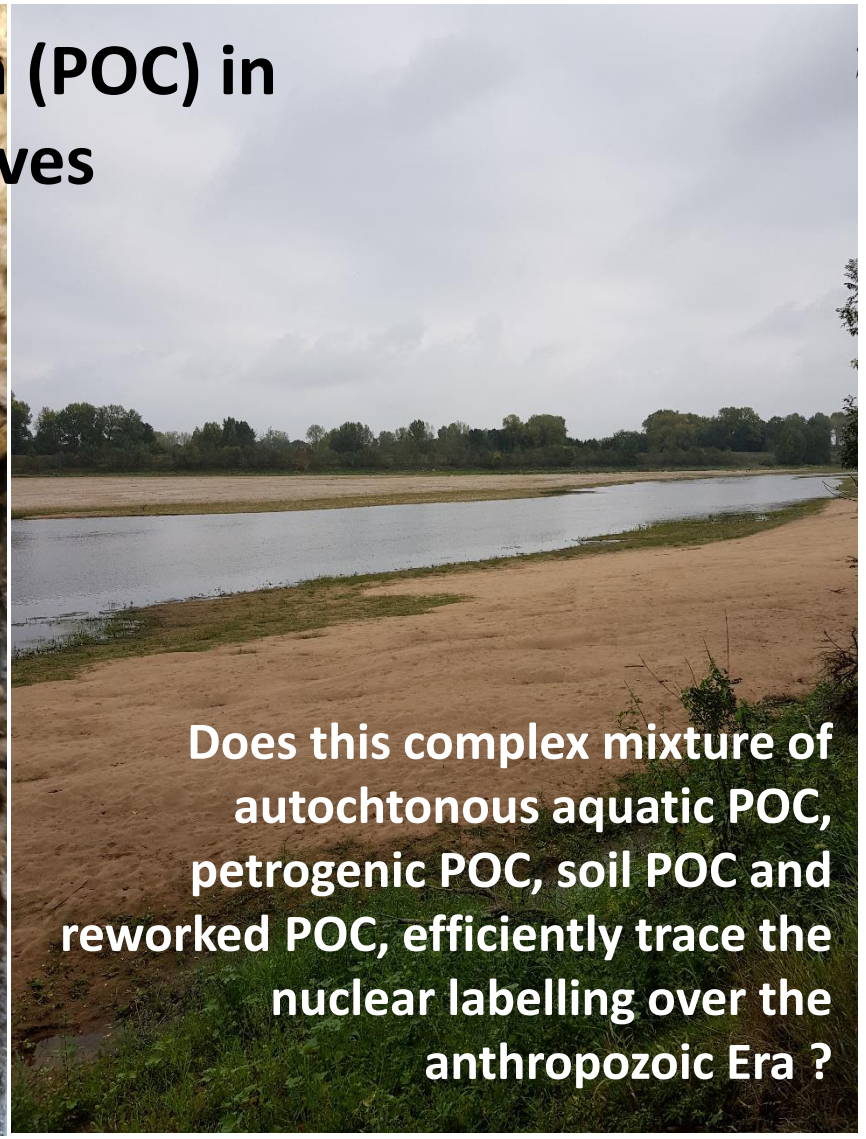

Does this complex mixture of autochtonous aquatic POC, petrogenic POC, soil POC and reworked POC, efficiently trace the nuclear labelling over the anthropozoic Era ?